Global Biogeochemical Cycles

RESEARCH ARTICLE
10.1029/2020GB006709

# Molecular Signatures of Glacial Dissolved Organic Matter From Svalbard and Greenland

**Anne M. Kellerman[1], Jorien Vonk[2,3], Stephanie McColaugh[1], David C. Podgorski[1,4], Elise van Winden[2], Jon R. Hawkings[1,5], Sarah Ellen Johnston[1,6], Munir Humayun[1], and Robert G. M. Spencer[1]**

[1]National High Magnetic Field Laboratory Geochemistry Group and Department of Earth, Ocean, and Atmospheric Science, Florida State University, Tallahassee, FL, USA, [2]Department of Earth Sciences, Utrecht University, Utrecht, The Netherlands, [3]Now at: Department of Earth Sciences, Vrije Universiteit Amsterdam, Amsterdam, The Netherlands, [4]Now at: Department of Chemistry, Chemical Analysis & Mass Spectrometry Facility, Pontchartrain Institute for Environmental Sciences, University of New Orleans, New Orleans, LA, USA, [5]German Research Centre for Geosciences GFZ, Potsdam, Germany, [6]Now at: Department of Biological Sciences, University of Lethbridge, Lethbridge, Canada

**Abstract** Glaciers and ice sheets cover over 10 % of Earth's land surface area and store a globally significant amount of dissolved organic matter (DOM), which is highly bioavailable when exported to proglacial environments. Recent rapid glacier mass loss is hypothesized to have increased fluxes of DOM from these environments, yet the molecular composition of glacially derived DOM has only been studied for a handful of glaciers. We determine DOM composition using ultrahigh resolution mass spectrometry from a diverse suite of Arctic glacial environments, including time series sampling from an ice sheet catchment in Greenland (Russell Glacier) and outflow from valley glaciers in catchments with varying degrees of glacial cover in Svalbard. Samples from the Greenland outflow time series exhibited a higher degree of similarity than glacier outflow between glaciers in Svalbard; however, supraglacial meltwater samples from Greenland and Svalbard were more similar to each other than corresponding glacial outflow. Outflow from Russell Glacier was enriched in polyphenolic formulae, potentially reflecting upstream inputs from plants and soils, or inputs from paleosols overridden by the ice sheet, whereas Svalbard rivers exhibited a high level of molecular richness and dissimilarity between sites. When comparing DOM compositional analyses from other aquatic systems, aliphatic, and peptide-like formulae appear particularly abundant in supraglacial meltwater, suggesting the DOM quickly metabolized in previous incubations of glacial water originates from energy-rich supraglacial sources. Therefore, as glaciers lose mass across the region, higher-quality fuel for microbial degradation will increase heterotrophy in coastal systems with ramifications for carbon cycling.

**Key Points:**

- Dissolved organic matter (DOM) exhibits compositional variability in glacial outflow across Svalbard and Greenland
- Supraglacial DOM is compositionally similar across glaciers in Svalbard and Greenland but distinct from subglacial outflow
- Glacial DOM is uniquely enriched in aliphatic and peptide-like organic matter compared to other aquatic systems

**Supporting Information:**

- Suppporting Information S1

**Correspondence to:**
A. M. Kellerman,
akellerman@fsu.edu

**Citation:**
Kellerman, A. M., Vonk, J., McColaugh, S., Podgorski, D. C., van Winden, E., Hawkings, J. R., et al. (2021). Molecular signatures of glacial dissolved organic matter from Svalbard and Greenland. *Global Biogeochemical Cycles*, *35*, e2020GB006709. https://doi.org/10.1029/2020GB006709

Received 12 JUN 2020
Accepted 18 JAN 2021



## 1. Introduction

Glaciers are a defining feature and active biome in polar and alpine environments, integrating biogeochemical and physical processes over large spatial areas (Anesio et al., 2017; Hodson et al., 2008). Although glacial mass has been steadily decreasing since the end of the Little Ice Age, ice mass loss has recently accelerated with anthropogenic climate change (Liao et al., 2014). Between 1991 and 2010, ~69% ± 24% of global glacier mass loss can be attributed to anthropogenic activities (Liao et al., 2014). This accelerated mass loss is projected to result in a decrease of ~15 Tg in glacial carbon (C) stores by 2050 (Hood et al., 2015). Consequently, glaciers will continue to act not only as long-term stores of C, but also as changing sources of organic matter to downstream environments (Hood et al., 2009, 2015; Wadham et al., 2019).

Dissolved organic matter (DOM) is a key modulator in the global carbon cycle (Battin et al., 2009). DOM is comprised of a heterogeneous mixture of molecules, predominantly originating from photosynthesis and diversified through partial decomposition. DOM plays a multifunctional role in the environment. For example, DOM forms the base of the microbial foodweb, serving as a substrate for heterotrophic communities, and also acts a natural protectant for microbial communities by absorbing UV irradiation (Findlay & Sinsabaugh, 2003). This is particularly true in supraglacial environments where substrates for heterotrophs are scarce, and algal and microbial communities are exposed to harsh levels of irradiance (Williamson et al., 2020). Reactivity has been linked to organic matter composition as well as environmental controls

(Kellerman et al., 2015; Schmidt et al., 2011), and DOM composition has been linked to the source of DOM. Glacial DOM sources include ancient organic matter previously stored cryogenically or held in subglacial stores, atmospheric deposition, and recently produced DOM in supraglacial and subglacial ecosystems (Hood et al., 2009; Spencer, Guo, et al., 2014; Spencer, Vermilyea, et al., 2014; Wadham et al., 2019). DOM characteristics have been shown to be indicative of hydrological evolution at a polythermal glacier, from outflow dominated by water interacting with the basal environment early in the melt season to supraglacial melt flowing through channelized drainage at peak melt (Kellerman et al., 2020b). Furthermore, spatial and temporal variability of dissolved organic carbon (DOC) concentrations have been observed over the ablation season on the Greenland Ice Sheet (GrIS) (Holland et al., 2019; Musilova et al., 2017), potentially due to increasing algal production with surface melt (Nicholes et al., 2019). Heterogeneous distribution of DOM on the ice surface may be reflected in what is exported from the supraglacial environment.

Fourier transform ion cyclotron resonance mass spectrometry (FT-ICR MS) has emerged as a valuable tool for analyzing the composition of DOM and has provided novel insights into our understanding of DOM sources, diversity, composition, and reactivity (Kellerman et al., 2014; Mostovaya et al., 2017; Noriega-Ortega et al., 2019). Precise assignment of molecular formulae allows for basic structural features to be deduced from elemental composition of the molecular formulae (Koch & Dittmar, 2006; Stenson et al., 2003). DOM in glacial environments has previously been shown to exhibit high contributions of aliphatic (H/C $>$ 1.5) and N-containing aliphatic formulae (i.e., peptide-like formulae) (Bhatia et al., 2010; D'Andrilli et al., 2015; Lawson, Bhatia, et al., 2014; Stubbins et al., 2012), however there is generally a paucity of glacial DOM compositional data, and a systematic comparison of glacial DOM to DOM in other environments has not been conducted. Elevated contributions from energy-rich aliphatic and peptide-like formulae have been postulated to contribute to the remarkably bioavailable DOC observed in glacial systems (Spencer, Guo, et al., 2014). Thus, understanding the spatial and temporal variability of DOM composition in glacial systems, as well as the sources of glacially derived DOM, is critical for determining the implications of climate change on glacial C cycling.

Here, we present DOC concentration and DOM composition from a time series of outflow (May 13–June 13, 2016) at Russell Glacier, a small land-terminating glacier of the GrIS, and a suite of 11 glacially fed rivers in Svalbard to establish a compositional baseline for glacial systems in the Arctic. Additionally, supraglacial samples were collected from both Greenland ($n$ = 3) and Svalbard ($n$ = 2) to examine compositional differences between supraglacial sources and subglacial or ice-marginal sources in the outflow. Lastly, we compared glacial DOM at our study sites to DOM in other glacier studies, non-glacial rivers, and marine environments. We hypothesize that DOM in glacial environments will be enriched in bioavailable aliphatic and peptide-like formulae, particularly in the supraglacial environment where there is limited potential for direct inputs from terrestrial sources (i.e., plants and soils), with clear ramifications for downstream ecosystems during ongoing glacier mass loss.

## 2. Materials and Methods

### 2.1. Sampling Sites

#### 2.1.1. Greenland Sampling Sites

Glacial outflow (proglacial) river samples were collected every two to four days between May 13 and June 13, 2016 ($n$ = 15), from the subglacially routed outlet of Russell Glacier (67.091°N, 50.240°W), a small outlet glacier of the GrIS (Table S1, Figure 1). Russell Glacier is estimated to have a catchment area of ~100 km$^2$ (Lindbäck et al., 2015; Rennermalm et al., 2013; Wal & Russell, 1994). A supraglacial pond was sampled twice and a supraglacial stream was sampled once during the sampling period (67.146°N, 50.022°W and 67.149°N, 50.010°W, respectively), both within 1.5 km of the GrIS margin (Table S1, Figure 1).

The outflow of Russell Glacier feeds into the Akuliarusiarsuup Kuua River, which is the northern tributary of Watson River. Watson River discharge ($Q$) was used to determine the timing of sampling during the melt season, even though Russell Glacier catchment only contributes a small amount to Watson River $Q$ (Rennermalm et al., 2012). Hourly and daily average Watson River meltwater $Q$ data from the 2016 melt season was retrieved from the Programme for Monitoring of the GrIS (PROMICE) database, where data points missing from the stage record were estimated from the air temperature (van As et al., 2017, 2019). Watson

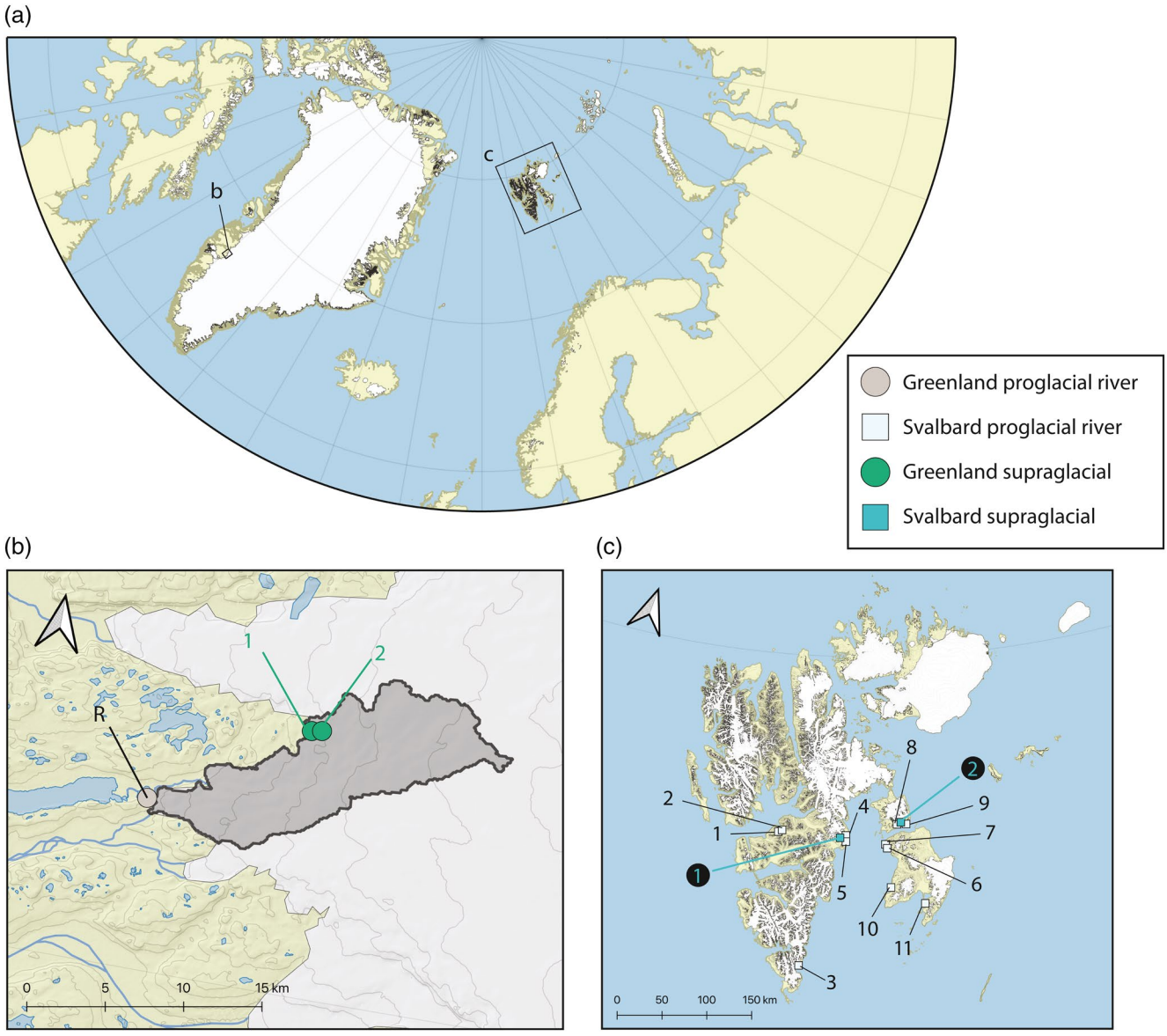


**Figure 1.** Map of the glacier study sites in Greenland and Svalbard (a). Russell Glacier, an outlet glacier of the Greenland Ice Sheet (GrIS) was sampled temporally (<0.05 km from the outlet; gray filled circle labeled as R and corresponding to GR1-15 in Table 1), and supraglacial melt sites were sampled within 0.5 km of each other (b; < 1.5 km from the GrIS margin; green filled circles labeled as 1 (GS1 and GS3) and 2 (GS2) are detailed in Table 1). The gray shaded area is the catchment area of Russell Glacier. Glacially fed streams (light blue filled squares) and glacier ice were sampled in Svalbard (c; turquoise squares). Black numbers correspond to SR1-11 and turquoise 1 and 2 on black-filled circles correspond to SS1 and SS2 in Table 1, respectively.

River meltwater $Q$ was gauged 0.15 km upstream of the Kangerlussuaq bridge, ~25 km downstream of the Russell Glacier portal.

### 2.1.2. Svalbard Sampling Sites

Sampling in Svalbard was conducted as part of the Dutch Scientific Research Expedition Edgeøya Svalbard (SEES) in August 2015. Glacially fed streams were sampled in Svalbard on the islands of Spitsbergen, Barentsøya, and Edgeøya across catchments with varying upstream glacier coverage. Glacier ice was sampled from the Ulvebreen and Freemanbreen glaciers on Spitsbergen and Barentsøya, respectively. Sampling locations can be found in Table S1 and Figure 1.

### 2.2. Sample Collection and Analysis

Water was collected in acid-washed (1.2 M HCl for >24 h) 1 L polycarbonate bottles and filtered through precombusted (450°C for 4 h) 47-mm glass microfiber filters with a 0.7 μm nominal pore size (Whatman GF/F). Filtered samples were stored frozen in 1 L polycarbonate bottles until they could be shipped frozen to the laboratory at Florida State University (USA) for further analysis.

#### 2.2.1. Dissolved Organic Carbon Concentration

Aliquots for DOC concentration and DOM composition analyses were acidified to pH 2 using 12 M HCl after samples were thawed. DOC concentration was determined using a Shimadzu TOC-L high-temperature catalytic oxidation total organic carbon analyzer. Nonpurgeable organic carbon was measured after sparging for 5 min at a flow rate of 80 ml $min^{-1}$. DOC concentrations were determined using a 6-point calibration curve. Replicate injections were averaged and had a coefficient of variance <4%.

#### 2.2.2. Fourier Transform Ion Cyclotron Resonance Mass Spectrometry

Samples for DOM compositional analyses were solid phase extracted (SPE) to normalize DOC concentrations across the data set and remove salts prior to FT-ICR MS. Samples were extracted onto PPL resin (Agilent Technologies), prepared using a modified version of the previously described protocol (Dittmar et al., 2008). Methanol (MeOH; MilliPore, HPLC grade) was used to condition 100 mg 3 mL PPL cartridges. PPL resin was soaked in MeOH for at least 4 h, before rinsing twice with ultrapure water, once with MeOH and twice with ultrapure water acidified to pH 2. After conditioning, acidified sample was passed over the cartridge with the volume adjusted by the DOC concentration in order to achieve a target elution concentration of 60 mg C $L^{-1}$. Cartridges were then rinsed twice with pH 2 ultrapure water and dried with ultrahigh purity $N_2$, before elution with 1 mL MeOH into 2 mL precombusted (550°C for 4 h) amber glass vials. Eluates were stored at −20°C until analysis on the FT-ICR MS.

DOM composition for the Greenland samples was analyzed using a custom-built 21 tesla FT-ICR MS, and DOM composition for the Svalbard samples was analyzed using a custom-built passively shielded 9.4 tesla FT-ICR MS at the National High Magnetic Field Laboratory in Tallahassee, Florida (Hendrickson et al., 2015; D. F. Smith et al., 2018). Negative ions were directly injected into the FT-ICR MS using electrospray ionization and at a flow rate of 0.7 μL $min^{-1}$. One hundred transients were co-added for each sample and signals less than the root mean square baseline plus 6$\sigma$ were not considered.

Mass spectra were calibrated using Predator Analysis software (Blakney et al., 2011), and singly charged ions between 170 and 1,000 Da were assigned molecular formulae within the bounds of $C_{1\text{-}100}H_{4\text{-}200}O_{1\text{-}25}N_{0\text{-}2}S_{0\text{-}1}$ and ± 0.5 ppm error using EnviroOrg (Corilo, 2015). Molecular formulae were classified by heteroatomic content as containing carbon, hydrogen and oxygen only (CHO), or with nitrogen (CHON), sulfur (CHOS), and both N and S (CHONS). Molecular formulae were also categorized based on their elemental ratios of H/C and O/C as well as the modified aromaticity index ($AI_{mod}$), which is calculated as

$$AI_{mod} = \frac{DBE_{AI}}{C_{AI}} = \frac{1 + C - \frac{1}{2}O - S - \frac{1}{2}(N + H)}{C - \frac{1}{2}O - N - S} \quad (1)$$

where C, H, O, N, and S are the number of carbon, hydrogen, oxygen, nitrogen, and sulfur atoms in a given molecular formula (Koch & Dittmar, 2006, 2016). Nominal oxidation state of carbon (NOSC) was calculated as

$$NOSC = 4 - \frac{(4C + H - 3N - 2O - 2S)}{C} \quad (2)$$

where C, H, O, N, and S denotes the number of atoms of each element in each formula (Riedel et al., 2012). Formulae were classified into six groups: condensed aromatics (CA; $AI_{mod} \geq 0.67$), polyphenolics (PP; $0.67 > AI_{mod} > 0.50$), highly unsatured and phenolic formulae (HUP; $AI_{mod} \leq 0.50$, $H/C < 1.5$), aliphatics ($H/C \geq 1.5$, $O/C \leq 0.9$, $N = 0$), peptide-like formulae ($H/C \geq 1.5$, $O/C \leq 0.9$, $N > 0$), and sugar-like formulae

(H/C ≥ 1.5, O/C > 0.9) (Osterholz et al., 2016; Spencer, Guo, et al., 2014). Relative abundance weighted metrics of the mass, $AI_{mod}$, NOSC, heteroatomic content (i.e., CHO, CHON, CHOS, CHONS), and formulae categories are reported in Table 1. In this study, we focus on changes in these metrics and relative abundance in formula categories, as this has shown to be most robust for comparisons across instruments (Hawkes et al., 2020; Zherebker et al., 2020). Suwanee River Fulvic Acid Standard (2S101F) showed < 2% difference in relative abundance of formula categories across instruments.

Structural features can be deduced from $AI_{mod}$ and elemental ratios (e.g., presence of a condensed aromatic core) (Koch & Dittmar, 2006), however each molecular formula may represent an unknown number of structural isomers (Hertkorn et al., 2007). Thus, the specific structural configuration of a molecular formula cannot be determined without further analysis. The categories therefore are operationally defined by $AI_{mod}$ and elemental ratios, and N-content in the case of the peptide-like group. Regardless, condensed aromatics and polyphenolics are conservatively categorized, as their $AI_{mod}$ necessitates the presence of condensed aromates or multiple aromatic structures, respectively (Koch & Dittmar, 2006). There are likely many compounds in the highly unsaturated and phenolic group that contain aromatic structures combined with aliphatic side chains and do not meet the minimum $AI_{mod}$ threshold to be grouped with polyphenolics (Koch & Dittmar, 2006). An example for glacial systems would be purpurogallin carboxylic acid-6-O-b-D-glucopyranoside, a pigment produced by glacier algae, where the purpurogallin contains an 2-ring aromatic core (Remias et al., 2012), but the glucopyranoside sidechain reduces the $AI_{mod}$ so that it would be conservatively categorized with the highly unsaturated and phenolic formulae. Regardless, these groups have been repeatedly demonstrated to show systematic and biogeochemical coherence with sources and degradation patterns of DOM (D'Andrilli et al., 2015; Kellerman et al., 2018; Spencer et al., 2015; Stubbins et al., 2010). Condensed aromatics and polyphenolics have been related to terrestrial sources of DOM including soil and plants (e.g., Kellerman et al., 2018) and are susceptible to photodegradation (e.g., Stubbins et al., 2010). Condensed aromatics, along with aliphatics, have also been associated to depositional sources of DOM (Stubbins et al., 2012; Wozniak et al., 2008). Formulae with high H/C (e.g., aliphatic, peptide-like, and sugar-like) have been associated with microbial and algal sources of DOM and high bioavailability (D'Andrilli et al., 2015; Kellerman et al., 2018; Spencer et al., 2015). Highly unsaturated and phenolic formulae comprise the remainder; they originate from multiple sources, often make up the majority of the relative abundance, the fraction of which increases with water residence time in freshwater systems (Kellerman et al., 2020a). Proposed structures range from degraded lignin to carboxylic-rich alicyclic molecules, a potentially recalcitrant fraction of DOM in the ocean (Hertkorn et al., 2006; Stenson et al., 2003).

#### 2.2.3. Cross-System Comparison of DOC Concentration and DOM Composition

Existing ultrahigh resolution mass spectrometry data was compiled from supraglacial samples, glacial outflow, marine systems, and non-glacial rivers to contextualize the composition of DOM in the samples presented here. Datasets were only included if DOC concentration and the ultrahigh resolution mass spectrometry derived compound categories of condensed aromatics, polyphenolics, aliphatics, and peptide-like or N-containing aliphatics were described. “Supraglacial samples” include ice, snow, and meltwater collected from the surface of the ice sheet or glacier. “Glacial outflow” included samples taken from proglacial rivers in catchments with >25% glacier coverage, “marine” was required to have salinity > 30 psu, and “non-glacial rivers” were required to have salinity < 0.5 psu, and <15% glacial contribution in headwaters.

#### 2.2.4. Statistical Analyses

All statistical analyses were executed in R (R Core Team, 2015). Relative abundance weighted metrics were calculated for the mass, $AI_{mod}$, and NOSC, as well as the formula categories listed in Section 2.2.2. Linear and semi-log regressions were calculated in R. Akaike's Information Criterion and visual inspection of residuals and leverage plots were used to assess the appropriateness of a log transformation for each model.

Where pairwise comparisons are reported, first an analysis of variance (ANOVA) not assuming equal variance was performed. Bartlett's test of homogeneity of variance was used to determine if variances were equal between groups. Groups included Greenland outflow samples, Svalbard river samples, and supraglacial samples from Greenland and Svalbard, which were pooled due to the limited sample size and compositional similarity. Variance was unequal between groups for all tests. Consequently, pairwise comparisons using a t-test that does not assume equal variance were assessed if the ANOVA was significant. A false

Global Biogeochemical Cycles

10.1029/2020GB006709

**Table 1**
*Dissolved Organic Carbon Concentrations and Dissolved Organic Matter Composition for Greenland and Svalbard Glaciers*

| | Date | DOC (mg C L-1) | Formulae (#) | Mass[a] | $AI_{mod}$[a] | NOSC[a] | Condensed aromatics (%RA) | Polyphenolic (%RA) | Highly unsaturated and phenolic (%RA) | Aliphatic (%RA) | Peptide-like (%RA) | Sugar-like (%RA) | CHO (%) | CHON (%) | CHOS (%) | CHONS (%) |
|---|---|---|---|---|---|---|---|---|---|---|---|---|---|---|---|---|
| Russell time series (Greenland) | | | | | | | | | | | | | | | | |
| GR1 | 13/05/2016 | 0.34 | 10,078 | 491.04 | 0.366 | 0.074 | 6.0 | 18.3 | 70.7 | 4.9 | 0.1 | 0 | 54 | 29 | 18 | 0 |
| GR2 | 15/05/2016 | 0.37 | 9,256 | 495.51 | 0.374 | 0.102 | 6.1 | 18.9 | 71.3 | 3.7 | 0.1 | 0.1 | 57 | 31 | 12 | 0 |
| GR3 | 17/05/2016 | 0.35 | 9,207 | 501.43 | 0.368 | 0.083 | 5.9 | 18.4 | 70.9 | 4.6 | 0.1 | 0 | 55 | 29 | 16 | 0 |
| GR4 | 19/05/2016 | 0.32 | 8,518 | 494.48 | 0.379 | 0.097 | 6.3 | 19.7 | 69.9 | 3.9 | 0.1 | 0 | 60 | 29 | 11 | 0 |
| GR5 | 23/05/2016 | 0.35 | 6,981 | 498.88 | 0.378 | 0.078 | 6.5 | 20.1 | 68.4 | 4.9 | 0.1 | 0 | 69 | 20 | 11 | 0 |
| GR6 | 25/05/2016 | 0.38 | 8,532 | 497.20 | 0.370 | 0.070 | 5.7 | 18.8 | 70.9 | 4.5 | 0.1 | 0 | 61 | 29 | 10 | 0 |
| GR7 | 28/05/2016 | 0.41 | 9,584 | 494.15 | 0.367 | 0.075 | 5.4 | 18.2 | 71.9 | 4.3 | 0.1 | 0 | 58 | 32 | 10 | 0 |
| GR8 | 30/05/2016 | 0.45 | 7,849 | 497.09 | 0.369 | 0.080 | 5.8 | 18.6 | 71.2 | 4.3 | 0 | 0 | 65 | 22 | 13 | 0 |
| GR9 | 01/06/2016 | 0.42 | 7,214 | 491.36 | 0.375 | 0.085 | 6.0 | 19.4 | 70.3 | 4.2 | 0.1 | 0 | 68 | 22 | 10 | 0 |
| GR10 | 03/06/2016 | 0.28 | 7,738 | 500.42 | 0.369 | 0.092 | 5.9 | 18.2 | 72.2 | 3.5 | 0.2 | 0.1 | 65 | 25 | 10 | 0 |
| GR11 | 05/06/2016 | 0.24 | 9,201 | 490.60 | 0.376 | 0.069 | 6.6 | 19.6 | 68.5 | 5.1 | 0.2 | 0 | 56 | 29 | 15 | 0 |
| GR12 | 07/06/2016 | 0.27 | 9,002 | 493.53 | 0.380 | 0.090 | 7.0 | 20.1 | 68.0 | 4.7 | 0.1 | 0 | 56 | 28 | 16 | 0 |
| GR13 | 09/06/2016 | 0.24 | 10,216 | 502.20 | 0.383 | 0.077 | 7.5 | 20.3 | 67.2 | 4.9 | 0.1 | 0 | 54 | 29 | 17 | 0 |
| GR14 | 11/06/2016 | 0.24 | 7,781 | 494.91 | 0.392 | 0.105 | 7.6 | 21.4 | 67.2 | 3.8 | 0 | 0 | 62 | 27 | 10 | 0 |
| GR15 | 13/06/2016 | 0.24 | 7,652 | 489.10 | 0.388 | 0.089 | 7.5 | 21.4 | 66.0 | 5.0 | 0.1 | 0 | 65 | 21 | 15 | 0 |
| Greenland supraglacial | | | | | | | | | | | | | | | | |
| GS1 | 22/05/2016 | 0.16 | 4,692 | 471.66 | 0.185 | −0.411 | 1.2 | 4.2 | 58.9 | 33.9 | 1.9 | 0 | 54 | 15 | 31 | 0 |
| GS2 | 08/06/2016 | 0.14 | 3,932 | 469.05 | 0.160 | −0.452 | 0.5 | 2.3 | 57.4 | 35.3 | 4.4 | 0 | 48 | 10 | 38 | 4 |
| GS3 | 11/06/2016 | 0.1 | 5,392 | 434.87 | 0.138 | −0.436 | 0.6 | 1.8 | 51.7 | 27.8 | 17.9 | 0.2 | 41 | 32 | 18 | 9 |
| Svalbard rivers | | | | | | | | | | | | | | | | |
| SR1 | 19/08/2015 | 0.17 | 13,321 | 400.38 | 0.432 | −0.081 | 12.3 | 24.5 | 58.6 | 4.4 | 0.2 | 0 | 33 | 36 | 20 | 10 |
| SR2 | 19/08/2015 | 0.23 | 13,758 | 410.10 | 0.368 | −0.208 | 8.0 | 18.2 | 64.2 | 8.0 | 1.5 | 0.1 | 34 | 38 | 19 | 9 |
| SR3 | 20/08/2015 | 0.15 | 11,811 | 388.04 | 0.217 | −0.397 | 3.1 | 6.9 | 55.6 | 27.9 | 6.4 | 0.2 | 34 | 41 | 19 | 6 |
| SR4 | 22/08/2015 | 0.1 | 7,335 | 379.86 | 0.258 | −0.480 | 3.4 | 9.7 | 53.7 | 28.3 | 4.7 | 0.1 | 45 | 37 | 18 | 0 |
| SR5 | 22/08/2015 | 0.12 | 8,816 | 367.61 | 0.269 | −0.234 | 2.2 | 8.5 | 71.1 | 15.8 | 2.0 | 0.4 | 38 | 32 | 25 | 5 |
| SR6 | 21/08/2015 | 0.19 | 15,870 | 419.53 | 0.306 | −0.226 | 5.1 | 11.3 | 70.1 | 10.6 | 2.7 | 0.1 | 33 | 41 | 19 | 7 |
| SR7 | 21/08/2015 | 0.51 | 11,566 | 400.30 | 0.282 | −0.227 | 2.3 | 7.9 | 77.6 | 11.2 | 0.8 | 0.1 | 37 | 34 | 21 | 8 |
| SR8 | 24/08/2015 | 0.16 | 12,828 | 397.39 | 0.235 | −0.362 | 3.9 | 8.0 | 56.6 | 27.1 | 4.2 | 0.1 | 35 | 37 | 21 | 7 |
| SR9 | 24/08/2015 | 0.24 | 15,641 | 413.17 | 0.324 | −0.144 | 6.1 | 13.2 | 67.7 | 10.9 | 1.9 | 0.1 | 28 | 40 | 21 | 11 |
| SR10 | 25/08/2015 | 0.1 | 8,521 | 382.86 | 0.273 | −0.360 | 3.0 | 8.0 | 69.2 | 16.5 | 3.2 | 0.1 | 42 | 44 | 14 | 0 |
| SR11 | 26/08/2015 | 0.14 | 9,620 | 403.96 | 0.297 | −0.238 | 4.2 | 9.7 | 74.9 | 10.2 | 0.8 | 0.1 | 46 | 34 | 20 | 1 |

**Table 1**
*Continued*

| | Date | DOC (mg C L-1) | Formulae (#) | Mass[a] | $AI_{mod}$[a] | NOSC[a] | Condensed aromatics (%RA) | Polyphenolic (%RA) | Highly unsaturated and phenolic (%RA) | Aliphatic (%RA) | Peptide-like (%RA) | Sugar-like (%RA) | CHO (%) | CHON (%) | CHOS (%) | CHONS (%) |
|---|---|---|---|---|---|---|---|---|---|---|---|---|---|---|---|---|
| Svalbard supraglacial | | | | | | | | | | | | | | | | |
| SS1 | 22/08/2015 | 0.51 | 2,663 | 336.87 | 0.188 | −0.573 | 2.2 | 5.7 | 41.0 | 37.4 | 13.5 | 0.2 | 66 | 34 | 0 | 0 |
| SS2 | 24/08/2015 | 0.54 | 3,140 | 338.20 | 0.163 | −0.612 | 2.2 | 6.0 | 31.8 | 41.4 | 18.5 | 0.1 | 52 | 37 | 11 | 0 |

Abbreviations: $AI_{mod}$, modified aromaticity index; CHO/N/S, formulae that contain combinations of carbon, hydrogen, oxygen, nitrogen and/or sulfur; DOC, dissolved organic carbon concentration; NOSC, nominal oxidation state of carbon.
[a]Indicates variables that are relative abundance weighted averages.

discovery rate *p*-value correction for multiple comparisons was also applied. A similar approach with ANOVAs and pairwise comparisons was used to determine differences between the four categories (supraglacial, glacial outflow, marine, and non-glacial rivers) to explore the unique characteristics of glacier-associated DOM.

Variables were standardized to a range of 0–1 before performing principal component analysis (PCA) using the community ecology package "vegan" (Oksanen et al., 2011). A dissimilarity matrix was generated on the standardized variables using Euclidean distances. For these two analyses, the percent relative abundance of the highly unsaturated and phenolic formulae group was separated into high and low O/C groups at O/C = 0.5 (HUPs, High O/C; HUPs, Low O/C).

## 3. Results and Discussion

### 3.1. Molecular Signatures of Glacially Fed Rivers

#### 3.1.1. Russell Glacier Outflow Into Akuliarusiarsuup Kuua River

During the sampling period (May 13–June 13, 2015), daily $Q$ ranged from 25 to 1100 $m^3\ s^{-1}$ downstream in Watson River, and $Q$ did not reached maximum values (>2000 $m^3\ s^{-1}$) until late July (Figure 2a), which is typical for Watson River (Rennermalm et al., 2012). DOC concentration in Russell Glacier outflow ranged from 0.24 to 0.45 mg C $L^{-1}$ averaging (mean ± s.d.) 0.33 ± 0.07 mg C $L^{-1}$ (Figure 2b, Tables 1 and 2). DOC concentration decreased with increasing downstream $Q$ (Table S2, $R^2 = 0.35$, $p < 0.05$). Low but variable $Q$ has been previously observed within the Watson River catchment from neighboring Leverett Glacier during the onset of melt period (i.e., as the ablation season begins) (Hatton et al., 2019; Kellerman et al., 2020b). Although the ablation season officially began on 10–12 May, the sampling campaign was punctuated by an intermediate period where the seven-day rolling average air temperature was near freezing. This resulted in decreased $Q$ in Watson River and a delay in the ramp up of the melt season (Figure 2a). Consequently, DOC concentrations in Russell Glacier outflow are similar to the higher concentrations observed in other land-terminating Greenlandic glaciers during the onset of melt (Bhatia et al., 2013; Kellerman et al., 2020b; Kohler et al., 2017). This is supported by the semi-log relationship between $Q$ and the seven-day rolling average of the air temperature (Table S2, $R^2 = 0.91$, $p < 0.001$), as $Q$ is primarily controlled by weather conditions over the ice sheet (Braithwaite, 1995; Cowton et al., 2012). As $Q$ and air temperature are strongly related, only relationships between composition and $Q$ are presented below.

Changes in DOM composition over the sampling period were small but dominated by variability in aromaticity (Figure 3). The number of molecular formulae, mass, and NOSC did not change appreciably with $Q$, and exhibited averages of 8,587 ± 1,018, 495 ± 4 Da, and 0.084 ± 0.011, respectively (Table 2). $AI_{mod}$ had an average of 0.376 ± 0.008 and increased with increasing $Q$ (Figure 3a, Table S2; $R^2 = 0.60$, $p < 0.001$). Similarly, the relative abundance of polyphenolics (19% ± 1%RA) and condensed aromatics (6% ± 1%RA) increased with increasing $Q$ (Figure 3b, Table S2). Highly unsaturated and phenolic compound relative abundance (70% ± 2%RA) decreased with increasing $Q$ (Figure 3c, Table S2). Aliphatic (4% ± 1%RA) and peptide-like formulae (0% ± 0%RA) did not change appreciably with $Q$ (Figure 3d). The increase of aromatic moieties with increasing $Q$ is likely a feature of the onset of melt period where subglacial waters are draining marginal areas beneath the ice sheet, and DOM composition exhibited characteristics that suggest sources from soils and higher plants, potentially from paleosols overridden by the margin of the ice sheet (Bhatia et al., 2010; Kellerman et al., 2020b). Although meltwater from the ice sheet is the predominant source of water in Akuliarusiarsuup Kuua River, the river transverses a > 12 km reach of tundra before joining the outflow from Russell Glacier where it was sampled (Rennermalm et al., 2012). This may have led to terrestrial overprinting masking some of the compositional signatures of subglacial waters emerging from Russell Glacier.

Despite the changes in aromaticity associated with $Q$, DOM composition in Russell Glacier outflow was relatively invariant. This can be observed by the clustering of Russell Glacier outflow samples in the PCA (Figure 4) and the high similarity among Russell Glacier outflow in the dissimilarity matrix (Figure 5). Russell Glacier outflow separates out from the other glacial rivers based on its high aromaticity and low heteroatomic content (Figure 4) and comprises one of the three main clusters in

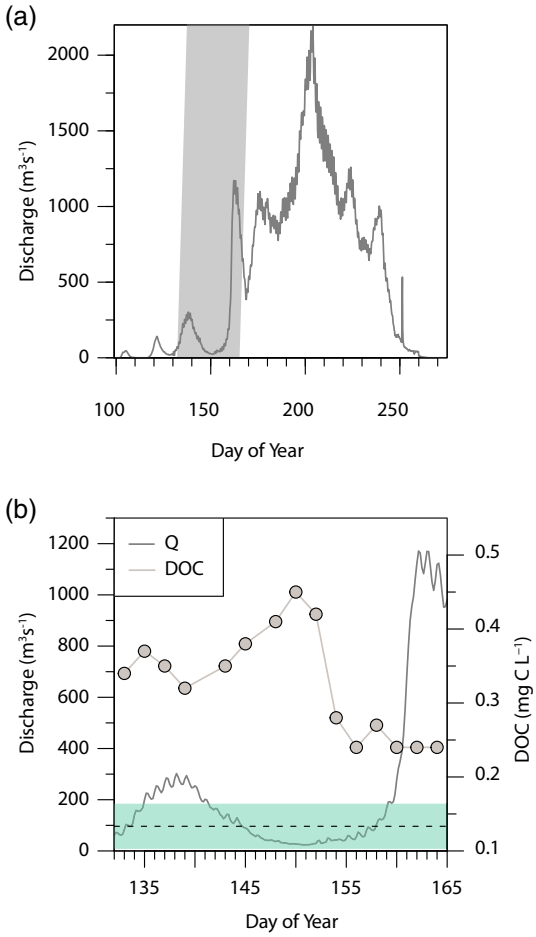


**Figure 2.** Hydrologic setting of Watson River watershed and timing of Russell Glacier sampling. Discharge ($Q$) from Watson River over the course of the melt season, which includes Russell Glacier $Q$ in its watershed (a). Vertical gray bar indicates timing of sampling at Russell Glacier, which is equivalent to the time period displayed in panel (b). Discharge in Watson River during the sampling period (dark gray line) and DOC concentrations over time in Russell Glacier outflow (b; gray filled circles). Horizontal dashed line and green band indicates the mean ± standard deviation of the DOC concentration in the supraglacial sites ($n = 3$). DOC, dissolved organic carbon.

the dissimilarity analysis (Figure 5). Low compositional variability has previously been observed during the onset of melt period at neighboring Leverett Glacier, suggesting that the dominant source of DOM does not change during this period (Kellerman et al., 2020b). Additionally, ice-marginal lakes are dynamic features along Russell Glacier (Knight et al., 2000), and the extent and volume of lakes along the western margin of the GrIS are increasing (Carrivick & Quincey, 2014). The ice-marginal lakes along Russell Glacier may cause DOM composition in Russell outflow to converge (i.e., temporally exhibit low compositional variability), as lakes have been shown to cause convergence of DOM composition with residence time (Kellerman et al., 2014).

### 3.1.2. Svalbard Rivers

Rivers in Svalbard ($n = 11$) were sampled during the peak of the melt season in August. DOC concentration in Svalbard rivers was low but variable (0.19 ± 0.12 mg C $L^{-1}$; Table 2, Figure S1). This is comparable to the DOC concentration found in outflow from mountain glaciers (0.37 ± 0.06 mg C $L^{-1}$, $n = 55$) (Hood et al., 2015) but lower than the DOC concentration in Svalbard fjords and coastal waters (0.50–0.72 mg C $L^{-1}$) (Osterholz et al., 2014; Paulsen et al., 2018). The DOC concentration in Svalbard rivers was significantly lower than that observed in early season Russell Glacier outflow ($p < 0.05$; Table 2).

There were distinct differences between DOM composition in Svalbard rivers and Russell Glacier outflow. The number of molecular formulae was higher in Svalbard rivers (11,735 ± 2,879) than in Greenland ($p < 0.01$; Table 2); whereas the mass (397 ± 16 Da; $p < 0.001$) and NOSC (−0.269 ± 0.118; $p < 0.001$) were lower in Svalbard rivers (Table 2). Generally, indices of aromaticity were lower in Svalbard rivers than in Greenland. $AI_{mod}$ (0.296 ± 0.061; $p < 0.01$) and polyphenolics (11% ± 5%RA; $p < 0.001$) were lower than in Russell Glacier outflow, however, there was no difference in the relative abundance of condensed aromatics (5 ± 3%RA; $p > 0.05$, Table 2, Figure S2). Aliphatic formulae were higher in Svalbard rivers (16 ± 9%RA) than in Greenland ($p < 0.001$). The relative abundance of highly unsaturated and phenolic formulae (65 ± 8%RA) and peptide-like formulae (3 ± 2%RA) were indistinguishable from Russell Glacier outflow ($p > 0.05$, Table 2, Figure S2). Additionally, the number of formulae that only contain carbon, hydrogen, and oxygen was higher in Russell outflow (60 ± 5%) than in the Svalbard rivers (37 ± 6%, Table 2; $p < 0.05$, Table 2).

The lower relative abundance of polyphenolic formulae and percent of CHO formulae in Svalbard rivers compared to Russell Glacier is likely due to differences in vegetation in upstream reaches of the rivers that were not sampled directly at the outflow. For example, the upstream catchment area of Akuliarusiarsuup Kuua River that is not overlain by the ice sheet is covered in mostly low shrub tundra and noncarbonate mountain complex, whereas glacier-free Svalbard landscapes are either barren or covered by smaller dwarf shrubs, grasses and mosses (CAVM Team, 2003). Furthermore, the western margin of the GrIS in the Kangerlussuaq region is postulated to be underlain by paleosols from growth during the last glacial minimum (Levy et al., 2017). The GrIS has active subglacial hydrology with extensive regions of saturated sediments (Jordan et al., 2018; MacGregor et al., 2016), which allows for microbial activity and may contribute more aromatic DOM signatures at the onset of melt (Kellerman et al., 2020b; O'Donnell et al., 2016). Svalbard glaciers, on the other hand, are a mixture of cold- and polythermal-based glaciers (Sevestre et al., 2015). Outflow from cold-based glaciers originates from direct supraglacial inputs and ice-marginal flow, whereas the warm bases of polythermal glaciers allow for the interaction of supraglacial water with the basal environment as it is routed through subglacial channels to the outflow portal (Irvine-Fynn et al., 2011). The variability in flowpaths and po-

**Table 2**
*Mean (Standard Deviation) and Analysis of Variance (ANOVA) Results for DOC Concentration and DOM Composition in This Study*

| Site type | | DOC (mg C $L^{-1}$) | Formulae (#) | Mass (Da) | $AI_{mod}$ | NOSC | Condensed aromatics (%RA) | Polyphenolics (%RA) | HUPs (%RA) | Aliphatics (%RA) | Peptide-like (%RA) |
|---|---|---|---|---|---|---|---|---|---|---|---|
| Mean (s.d.) | | | | | | | | | | | |
| Greenland river | n = 15 | 0.33 (0.07) | 8,587 (1,018) | 495 (4) | 0.376 (0.008) | 0.084 (0.011) | 6 (1) | 19 (1) | 70 (2) | 4 (1) | 0 (0) |
| Svalbard rivers | n = 11 | 0.19 (0.12) | 11,735 (2,879) | 397 (16) | 0.296 (0.061) | −0.269 (0.118) | 5 (3) | 11 (5) | 65 (8) | 16 (9) | 3 (2) |
| Supraglacial | n = 5 | 0.29 (0.22) | 3,964 (1,112) | 410 (68) | 0.167 (0.020) | −0.497 (0.090) | 1 (1) | 4 (2) | 48 (12) | 35 (5) | 11 (8) |
| ANOVA results | | | | | | | | | | | |
| One-way ANOVA | | 5.4 | 42 | 200 | 240 | 140 | 70 | 140 | 9.1 | 95 | 14 |
| Significance level | | * | *** | *** | *** | *** | *** | *** | ** | *** | ** |
| Greenland river | n = 15 | A | B | A | A | A | A | A | A | C | B |
| Svalbard rivers | n = 11 | B | A | B | B | B | A | B | A | B | B |
| Supraglacial | n = 5 | AB | C | AB | C | C | B | C | B | A | A |
| Significance level for pairwise comparisons | | * | ** | *** | ** | ** | ** | ** | * | ** | * |

Abbreviations: $AI_{mod}$, modified aromaticity index; DOC, dissolved organic carbon concentration; HUPs, highly unsaturated and phenolic formulae; NOSC, nominal oxidation state of carbon; %RA, percent relative abundance.
$^{*}p < 0.05$, $^{**}p < 0.05$, $^{***}p < 0.001$.

tential sources for each glacier may further explain the larger compositional variance in Svalbard rivers, compared to the similarity of outflow from Russell Glacier (Figures 4 and 5). The DOM of Russell Glacier outflow and Svalbard rivers is compositionally distinct, with Svalbard rivers forming a second major cluster in the dissimilarity analysis (Figure 5), despite high compositional variability among Svalbard rivers.

The number of molecular formulae is significantly higher in Svalbard rivers than in Russell Glacier outflow (Table 2, Figure 4). A higher fraction of heteroatomic formulae was found in Svalbard rivers (Table 2, Figure 4). The percent of N-containing formulae (CHON) and S-containing formulae (CHOS) were significantly higher in Svalbard rivers (CHON: 38 ± 4%, CHOS: 20 ± 3%) than in Russell outflow (CHON: 27 ± 4%, CHOS: 13 ± 3%) ($p < 0.001$, for both variables). Formulae containing both N and S (CHONS) averaged 6 ± 4% of formulae in Svalbard rivers but were not detected in any of the Russell outflow samples (Table 1). This enrichment along with lower aromaticity in Svalbard rivers results in a compositional distinction between Russell outflow and Svalbard rivers (Figures 4 and 5). There are two likely explanations for the higher contributions from heteroatomic formulae in Svalbard rivers. First, Svalbard rivers are more likely to include ice-marginal inputs from supraglacial melt (see Section 3.2 for discussion on heteroatomic content of supraglacial samples). Second, DOM may be incorporated from direct weathering of the bedrock, and differences in the lithology of the two regions are considerable. While the GrIS in the Kangerlussuaq region is underlain by Precambrian Shield gneiss and granite (Bouysse, 2014), Svalbard bedrock in the region of the study glaciers is a mixture of sedimentary rock, including sandstone, siltstone, shale, bituminous shale, and coal seams (Norwegian Polar Institute, 2016). Kerogen, for example, has been shown to have extractable organic matter than is rich in CHON and CHOS formulae (Kamga et al., 2014; Salmon et al., 2011). While kerogen itself is insoluble in water and would need to be oxidized by biological or physicochemical processes to produce water soluble organic matter, kerogen and other organic matter within this organic-rich sedimentary bedrock may contribute to the significantly higher CHON and CHOS content in the Svalbard rivers as they travel either through subglacial or ice-marginal flowpaths.

### 3.2. Molecular Signatures of Supraglacial Dissolved Organic Matter

Supraglacial samples exhibited the largest range in DOC concentrations overall, from the lowest DOC concentrations observed in supraglacial sites in Greenland (0.10 mg C $L^{-1}$) to the highest concentrations observed in supraglacial ice in Svalbard (0.54 mg C $L^{-1}$; Table 1). Consequently, the DOC concentration in supraglacial sites was not significantly different from the glacially fed rivers in Greenland and Svalbard.

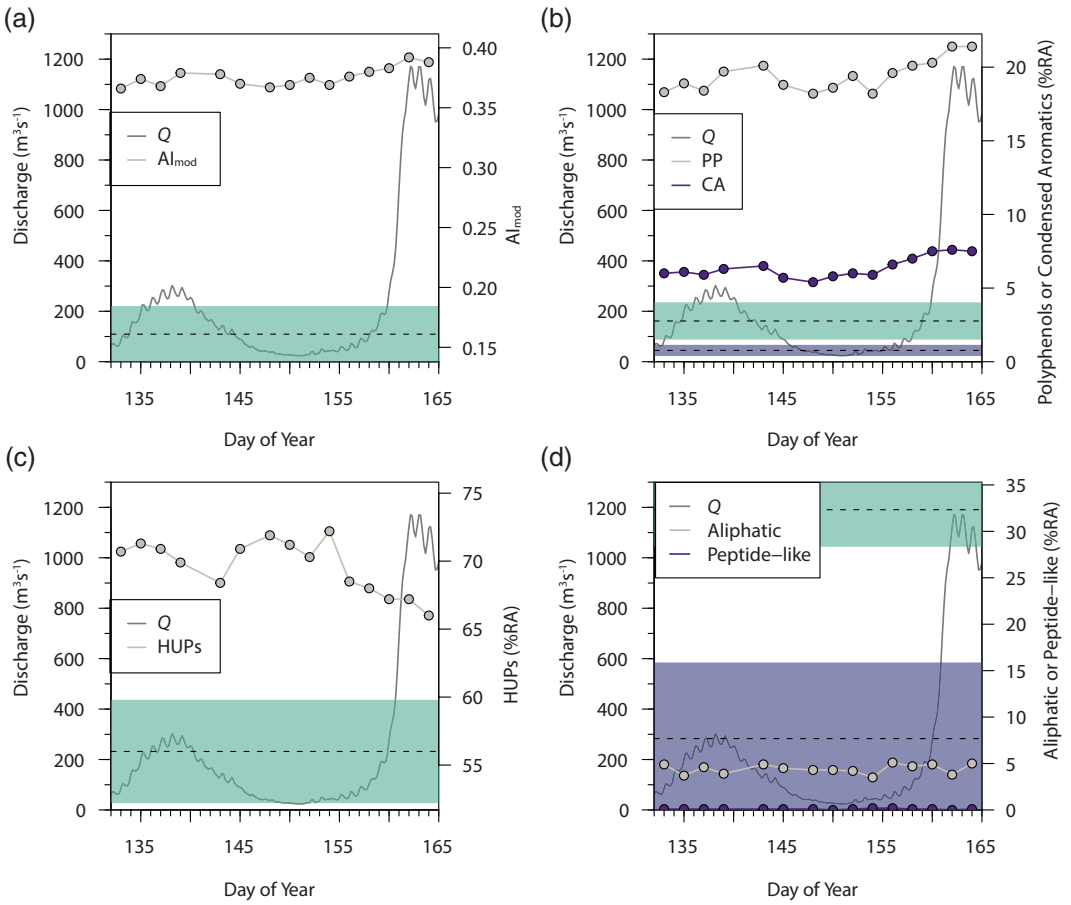


**Figure 3.** Temporal changes in molecular composition at Russell Glacier. Discharge ($Q$) in Watson River during the sampling period (dark gray line) and $AI_{mod}$ (a; gray filled circles), polyphenolic compounds (b; PP; gray filled circles), condensed aromatic compounds (b; CA; purple filled circles), highly unsaturated and phenolic compounds (c; HUPs; gray filled circles), aliphatic compounds (d; gray filled circles), and peptide-like compounds (d; purple filled circles) over time in Russell Glacier outflow. Horizontal bands indicate the mean ± standard deviation of $AI_{mod}$, PP, HUPs, and aliphatic formulae (green) and CA and peptide-like (purple) in the supraglacial sites ($n = 3$).

These DOC concentrations are consistent with previous measurements from supraglacial systems on the GrIS (Bhatia et al., 2010; Lawson, Wadham, et al., 2014; Musilova et al., 2017) and in mountain glaciers (Hood et al., 2015; Singer et al., 2012; Spencer, Guo, et al., 2014), and reflect the spatial heterogeneity of the supraglacial environment (Holland et al., 2019).

From a compositional perspective, supraglacial samples exhibited much lower molecular diversity in terms of the number of molecular formulae (3,964 ± 1,112) compared to the Greenland and Svalbard proglacial rivers ($p < 0.01$, for each comparison; Table 2). Despite the limited sampling size, there was a clear disconnect between the DOM composition in supraglacial samples across sites and the glacially fed rivers (Figure 4), with the supraglacial samples from Greenland and Svalbard forming the third major cluster in the dissimilarity matrix (Figure 5). $AI_{mod}$ (0.167 ± 0.020) and NOSC (−0.497 ± 0.090) were both significantly lower in supraglacial samples than in the river samples ($p < 0.01$, for each comparison; Table 2), reflecting the higher relative abundance of more saturated molecular formulae, regardless of oxygenation. This pattern is consistent throughout the compound groups, where the more unsaturated groups—condensed aromatics (1% ± 1%RA), polyphenolics (4 ± 2 %RA) and highly unsaturated and phenolic compounds (48% ± 12%RA)—were lower in relative abundance compared to Greenland and Svalbard proglacial rivers (Table 2).

Aliphatic (35% ± 5%RA) and peptide-like compounds (11% ± 7%RA) are more abundant in the supraglacial samples (Table 2). The degree of enrichment is particularly distinct for supraglacial DOM (Figure 6)

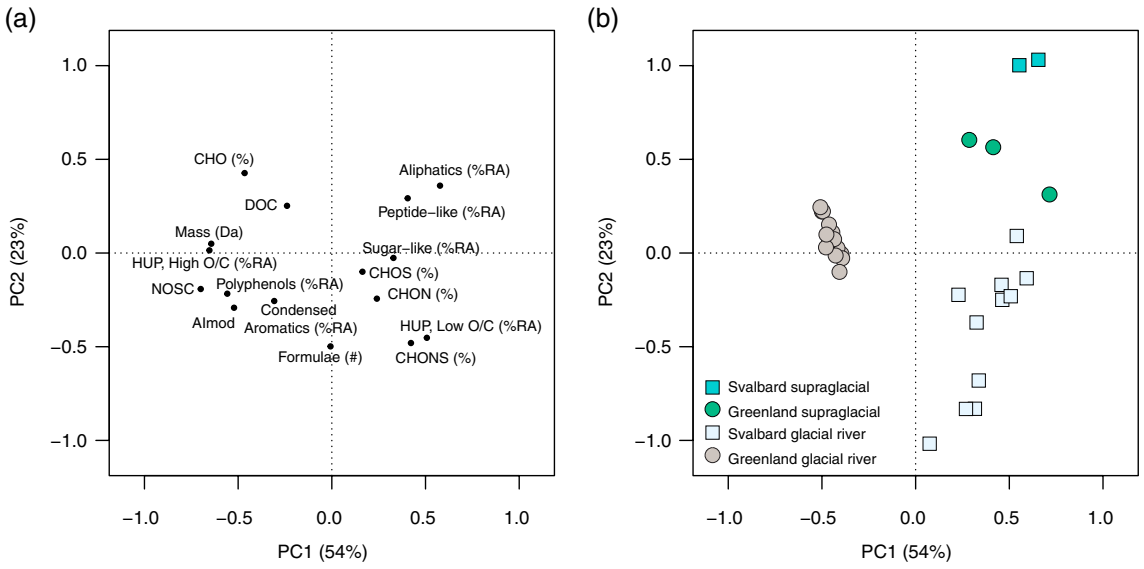


**Figure 4.** Principal component analysis of dissolved organic matter composition in Arctic glacial rivers. Loadings plot of the different variables (a) and the scores plot (b) of the samples from Greenland (Russell time series: gray filled circles; and supraglacial sites: green filled circles) and Svalbard (glacial rivers: light blue filled squares; and supraglacial sites: turquoise filled squares).

and is consistent with previous studies of supraglacial organic matter in polar and alpine biomes across continents (Bhatia et al., 2010; D'Andrilli et al., 2015; Lawson, Bhatia, et al., 2014; Singer et al., 2012; Stubbins et al., 2012). Surface ice environments are inhabited by extensive microbial communities, particularly glacier algae, that produce pigmentation as a mechanism to generate shade and liquid water, protecting themselves from the extreme irradiance conditions and the diurnal freeze-thaw cycles on the surface of the ice sheet (Dial et al., 2018; Remias et al., 2012; Williamson et al., 2018, 2020). The density of these microbial communities is spatially heterogeneous (Tedstone et al., 2017), as are the concentrations of exuded DOC, from highest in ice with high visible impurities to lowest in clean ice, supraglacial streams, and cryoconite holes (Holland et al., 2019). Bacteria have been found to tightly cycle freshly produced DOM in a supraglacial stream in Antarctica, exuding an excess of 2.17 μg C $L^{-1}$ $d^{-1}$ (Smith et al., 2017), similar to the rate of increase observed in supraglacial streams on the GrIS (Musilova et al., 2017). The balance between autotrophy and heterotrophy (i.e., rate of excess DOC production) in cryoconite holes is dependent on the size of the hole and sediment thickness, where small holes with thin sediment are net autotrophic and larger holes with thicker sediment are net heterotrophic (Cook et al., 2010; Telling et al., 2012). The enrichment of aliphatic and peptide-like compounds may be further enhanced by photo-degradation processes, which can degrade DOM with conjugated pi-systems and other DOM through indirect photodegradation and produce aliphatic photoproducts (Stubbins et al., 2010).

DOM produced by primary and secondary production in the supraglacial environment, including reworking of depositional OM, can be considered the exometabolome of the microbial community. A combination of cyanobacteria and glacier algae dominate primary production on the GrIS (Williamson et al., 2019). Heterotrophic communities, particularly in cryoconite holes (Nicholes et al., 2019; Stibal, Schostag, et al., 2015), can utilize such exudates and further diversify the microbial exometabolome (Wienhausen, 2018). Highly complex mixtures of thousands of molecular formulae detected using ultrahigh resolution mass spectrometry can be produced by individual strains of bacteria, such as *Pseudovibrio* and Roseobacter, even when grown on a simple, or even a single carbon source (Noriega-Ortega et al., 2019; Romano et al., 2014; Wienhausen et al., 2017), and could alone account for the richness of molecular formulae observed in the supraglacial samples (Table 2). Complex exometabolomes have been observed for cyanobacteria (Bittar et al., 2015; Fiore et al., 2015), Archaea (Bayer et al., 2019), brown macroalgae (Powers et al., 2019), and microalgae (Longnecker et al., 2015). Generally, the exometabolomes of microorganisms are enriched in aliphatic and heteroatomic elements (i.e., nitrogen and sulfur) (Fiore et al., 2015; Noriega-Ortega et al., 2019), which supports the enrichment of these formulae in the supraglacial samples from Svalbard and Greenland. Addi-

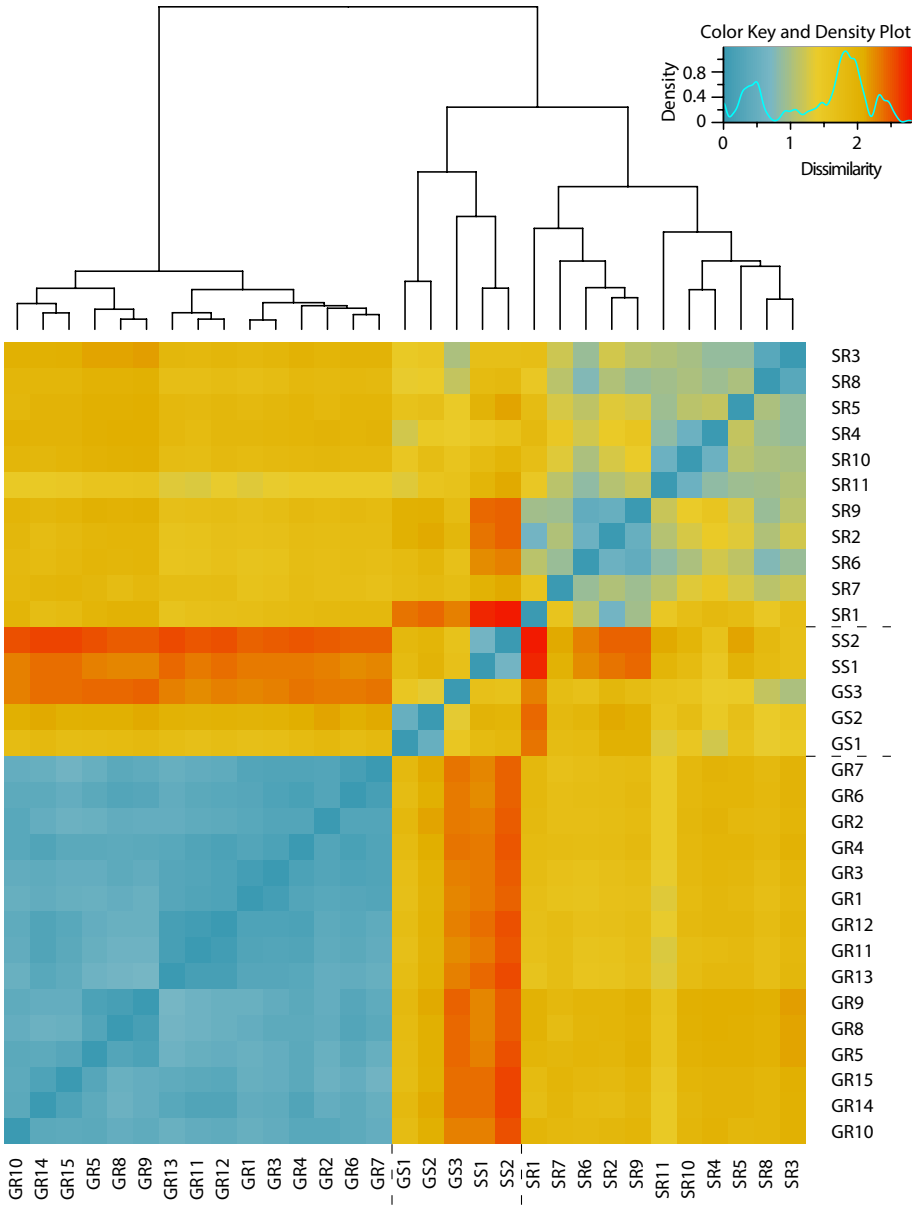


**Figure 5.** Dissimilarity matrix of samples from glacial rivers and supraglacial sites in Greenland and Svalbard based on Euclidean dissimilarity. Blue indicates sites that are highly similar and red indicates sites that are highly dissimilar.

tionally, formulae that positively correlate with chlorophyll *a* in an estuary study were enriched in nitrogen and sulfur (Osterholz et al., 2016), suggesting CHON and CHOS formulae are released during primary production, consistent with the high contributions of CHON and CHOS formulae in the supraglacial samples (Table 2).

Atmospheric deposition has also been proposed as an important source of DOM to the supraglacial environment, the types of which range from historic and current anthropogenic burning of fossil fuels and biomass, natural burning of biomass, to dust from regional sources and further afield (Moroni et al., 2018; Singer et al., 2012; Stubbins et al., 2012; Takeuchi et al., 2018; Wientjes et al., 2011). The apparent age of dust in the dark zone of the GrIS suggests that much of the dust was deposited during the Holocene interglacial period (Wientjes et al., 2017). Water soluble organic carbon from dry deposition is enriched in protein-like fluorescence (Mladenov et al., 2010, 2011), low molecular weight organic acids (Jacobson et al., 2000), and molecular formulae with H/C > 1.5 enriched in nitrogen and sulfur (Mazzoleni et al., 2012; Wozniak

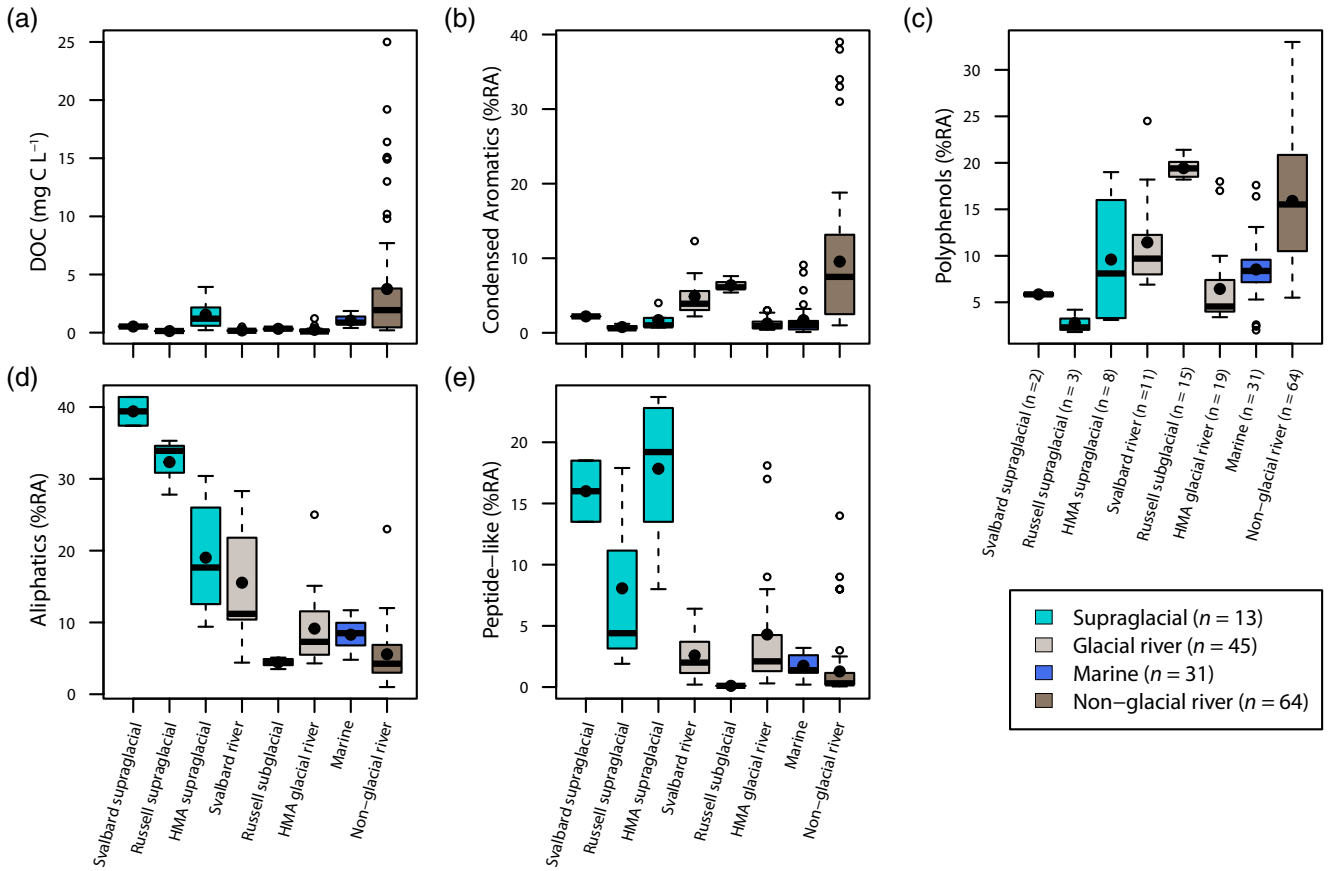


**Figure 6.** Comparison of DOC concentrations (a) and DOM composition (b–e) among supraglacial (turquoise), glacial (gray), marine (blue), and non-glacial rivers (brown). Svalbard and Russell data are from this study. The number of samples in each group is noted in the *x*-axis labels of panel (c). Statistical comparisons can be found in Table 3. Studies that contributed data to the different groups in the meta-analysis are marked as follows: supraglacial (s), glacial (g), marine (m), and non-glacial rivers (r). Chen et al. (2019) (r); Hemingway et al. (2019) (s,g,r); Kellerman et al. (2018) (m,r); Osterholz et al. (2016) (m,r); Riedel et al. (2016) (r); Seidel et al. (2015) (m,r); Spencer, Guo, et al. (2014) (s,g); Stubbins & Dittmar (2015) (m); Wagner et al. (2015) (r); Zhou, Zhou, Hu, et al. (2019) (s,g,r); and Zhou, Zhou, He, et al. (2019) (s,g). HMA, High Mountain Asia.

et al., 2008). Thus, deposition of organic matter could contribute to the enrichment of aliphatic and peptide-like formulae found in the supraglacial environment (Figure 6). Additionally, deposition of dust is an important source of inorganic nutrients to the supraglacial communities (Stibal, Gozdereliler, et al., 2015; Tedstone et al., 2017), thus deposition has a two-fold effect on the composition of DOM in the supraglacial environment (i.e., direct input and stimulation of primary/secondary production).

### 3.3. Unique Signatures of Glacial Dissolved Organic Matter

Data were compiled from other glacial systems, marine systems and non-glacial rivers to contextualize the composition of glacially derived DOM in this study (see list of references in Table 3 legend; Figure 6). Data were only included if the study reported DOC concentration as well as the compound categories condensed aromatics, polyphenolics, aliphatics, and peptide-like or N-containing aliphatic formulae (Table 3; Figure 6). Glacial studies were therefore limited to this study and five recent studies conducted in High Mountain Asia (HMA) (Chen et al., 2019; Hemingway et al., 2019; Spencer, Guo, et al., 2014; Zhou, Zhou, He, et al., 2019; Zhou, Zhou, Hu, et al., 2019). Data included in the non-glacial rivers span small to large watersheds, tropical to Arctic, low to high-DOC rivers, and allow us to compare DOM composition from glacial systems to a globally relevant range of rivers (references in Table 3). However, direct space-for-time comparisons to non-glacially influenced systems in Greenland and Svalbard may reveal how riverine DOM composition will change with deglaciation while taking into account region-specific characteristics such as climate and geology.

**Table 3**
*Mean (Standard Deviation) and Analysis of Variance (ANOVA) Results for DOC Concentration and DOM Composition in Meta-Analysis*

| Site type | | DOC (mg C $L^{-1}$) | Condensed aromatics (%RA) | Polyphenolics (%RA) | Aliphatics (%RA) | Peptide-like (%RA) |
|---|---|---|---|---|---|---|
| Mean (s.d.) | | | | | | |
| Supraglacial[a] | n = 13 | 0.62 (0.66) | 2 (1) | 7 (6) | 28 (10) | 14 (7) |
| Glacial outflow[a] | n = 45 | 0.23 (0.13) | 4 (3) | 12 (7) | 9 (6) | 2 (2) |
| Glacial outflow (excluding Russell Glacier)[a] | n = 30 | 0.18 (0.13) | 3 (3) | 8 (5) | 11 (7) | 3 (2) |
| Marine | n = 31 | 1.1 (0.4) | 2 (2) | 9 (3) | 8 (2) | 2 (1) |
| Non-glacial rivers | n = 64 | 3.8 (5.3) | 10 (9) | 16 (6) | 5 (3) | 1 (2) |
| ANOVA results | | | | | | |
| One-way ANOVA | | 43 | 20 | 19 | 20 | 16 |
| Significance level | | *** | *** | *** | *** | *** |
| Supraglacial[a] | n = 13 | BC | C | C | A | A |
| Glacial outflow[a] | n = 45 | C | B | B | B | B |
| Marine | n = 31 | B | C | C | B | B |
| Non-glacial rivers | n = 64 | A | A | A | C | B |
| Significance level for pairwise comparisons | | *** | *** | * | ** | *** |

*Notes*. Letters indicate where sample types are significantly different from each other in descending order from highest average value (A) to lowest (B or C). Significance levels are marked by one ($p < 0.05$), two ($p < 0.01$), or three asterisks ($p < 0.001$). Studies that contributed data to the different groups in the meta-analysis are marked as follows: supraglacial(s), glacial (g), marine (m), and non-glacial rivers (r). Chen et al. (2019) (r); Hemingway et al. (2019) (s,g,r); Kellerman et al. (2018) (m,r); Osterholz et al. (2016) (m,r); Riedel et al. (2016) (r); Seidel et al. (2015) (m,r); Spencer, Guo, et al. (2014) (s,g); Stubbins & Dittmar (2015) (m); Wagner et al. (2015) (r); Zhou, Zhou, Hu, et al. (2019) (s,g,r); and Zhou, Zhou, He, et al. (2019) (s,g).

Abbreviations: DOC, dissolved organic carbon concentration; HUPs, highly unsaturated and phenolic formulae; %RA, percent relative abundance.

[a]Includes data from this study.

The overall ANOVAs for each DOC concentration, condensed aromatics, polyphenolics, aliphatics, and peptide-like or N-containing aliphatic formulae among supraglacial, glacial outflow, marine and non-glacial rivers were significant with $p < 0.001$. Different systems exhibited heterogeneous variance largely due to high variability in DOC concentration and contribution of condensed aromatics and polyphenolics in the non-glacial rivers, and the high variability of aliphatics and peptide-like formulae in supraglacial samples (Table 3, Figure 6). Consequently, ANOVAs and pairwise comparisons not assuming equal variance were applied.

Glacial systems, both glacial outflow and supraglacial, are characterized by low DOC concentration (Figure 6a; Table 3). Glacial outflow exhibited the lowest DOC concentrations overall (0.23 ± 0.13 mg C $L^{-1}$, $n = 45$). Supraglacial DOC concentration was indistinguishable from both glacial outflow and marine systems due to the high variability observed in the wide range of supraglacial environments (low DOC concentration supraglacial streams to high DOC concentrations in dirty ice), but glacial outflow and marine DOC concentration were significantly different from each other (Table 3). Non-glacial rivers exhibited the highest average DOC concentrations, despite high variability (Figure 6a; one-way ANOVA and pairwise comparisons where significant were all < 0.001, Table 3). Marine samples selected for comparison are predominantly from coastal regions, and thus the DOC concentrations are skewed slightly high (1.1 ± 0.40 mg C $L^{-1}$, $n = 31$) compared to concentrations typical of the surface (0.84 mg C $L^{-1}$) and deep ocean (0.41 mg C $L^{-1}$) (Hansell et al., 2009). However, our marine samples do include both surface and deep water samples from both the Atlantic and Pacific Oceans (Kellerman et al., 2018; Osterholz et al., 2016; Seidel et al., 2015; Stubbins & Dittmar, 2015).

DOM composition of glacial systems was characterized by overall low relative contributions from aromatic formulae and high contributions from aliphatic and peptide-like formulae (Figure 6; Table 3). Samples from supraglacial and marine environments had the overall lowest contributions from condensed aromatics and polyphenolics and were not statistically distinct from one another (Figures 6b and 6c, Table 3).

Contributions from condensed aromatics and polyphenolics were higher in glacial outflow than marine and supraglacial samples ($p < 0.01$, for each comparison), with non-glacial rivers exhibiting the highest contributions from condensed aromatics and polyphenolic compounds (Figures 6b and 6c; $p < 0.001$, Table 3). This pattern is due to differing sources of DOM, but also likely due to differences in the importance of photodegradation in the different environments. Non-glacial rivers are typically dominated by known sources of aromatic compounds such as organic-rich soils and wetlands (Aitkenhead & McDowell, 2000; Spencer et al., 2012), particularly during high discharge (Casas-Ruiz et al., 2020). Glacial outflow may similarly be influenced by ice-marginal inputs, paleosols, and subglacial microbial production of DOM (Beaton et al., 2017; Lamarche-Gagnon et al., 2019), as photo-labile DOM can accumulate in dark environments (Stubbins & Dittmar, 2015). In comparison, supraglacial and marine environments are similarly dominated by microbial sources of DOM, with DOM in the marine surface impacted by photodegradation. Marine environments, and likely supraglacial environments, are heavily shaped by photo-oxidation (Hansell et al., 2009). Thus, even though microbial communities produce phenolic compounds, these compounds will be subjected to intense photodegradation on the highly irradiated ice surface (Remias et al., 2012; Williamson et al., 2020). This therefore leads to a convergence of DOM composition away from condensed aromatic structures (Kellerman et al., 2018). Estuarine environments can further exert compositional non-conservative changes to DOM through a variety of mechanisms, including photodegradation, flocculation, and algal and microbial production (Osterholz et al., 2016; Seidel et al., 2015).

Supraglacial environments consistently exhibited the highest contributions from aliphatic and peptide-like formulae of all environments despite variability in DOC concentration ($p < 0.001$, Table 3). Aliphatic compound contribution was higher in glacial outflow than marine, and lowest in non-glacial rivers ($p < 0.001$, for all comparisons). Peptide-like formulae were not significantly different between glacial outflow, marine, and non-glacial rivers ($p > 0.05$, for all comparisons; Table 3). Russell Glacier outflow was sampled early in the melt season, likely resulting in limited supraglacial inputs from the highly productive "dark zone" of the ice sheet surface (see Section 3.1). If Russell Glacier outflow is excluded from the ANOVA, glacial outflow exhibits higher peptide-like and aliphatic contributions than marine systems and non-glacial rivers ($p < 0.05$), and polyphenolics and condensed aromatics in glacial rivers are no longer significantly different from marine and supraglacial sites ($p > 0.05$). Aliphatic and peptide-like contributions are far more variable in glacial systems than in marine and non-glacial environments. This is particularly true for the supraglacial environment, even in High Mountain Asia samples from other studies (Chen et al., 2019; Hemingway et al., 2019; Spencer, Guo, et al., 2014; Zhou, Zhou, He, et al., 2019; Zhou, Zhou, Hu, et al., 2019).

The high protein-like fluorescence in both depositional and microbially produced DOM (Mladenov et al., 2011; Musilova et al., 2017) and high spatial and temporal variability in DOC concentration in the supraglacial environment (Holland et al., 2019; Musilova et al., 2017) make deconvoluting large scale controls on DOM composition problematic with the data at hand. Consideration also needs to be given to the timing of sampling during the melt seasons for supraglacial systems, as well as in glacial outflow that has temporally and spatially variant upstream inputs (Kellerman et al., 2020b). The wide range of supraglacial sample types (snow, ice, cryoconite holes, and supraglacial rivers and ponds) and microbial production over the course of the ablation season, result in spatially and temporally heterogeneous DOC concentrations (Holland et al., 2019; Musilova et al., 2017). Presumably this spatial and temporal heterogeneity also holds for DOM composition, creating further opportunities for sampling bias. Regardless, low DOC concentration, low relative abundance of condensed aromatic and polyphenolic formulae, and high relative contributions from aliphatic and peptide-like formulae characterize glacial systems.

### 3.4. Implications for Downstream Ecosystems in a Warming World

Seasonal differences in compositional export from glaciers from onset of melt to peak discharge have previously been reported for both organic and inorganic material (e.g., Bhatia et al., 2013; Hawkings et al., 2017; Kellerman et al., 2020b; Spencer, Vermilyea, et al., 2014). Despite differences in seasonality in our data set, where only onset of melt is available from Russell Glacier and synoptic samples from peak discharge in Svalbard rivers, a clear difference between DOC concentration and DOM composition can be observed between glacial systems, autochthonously dominated DOM in marine systems and terrestrially dominated DOM in non-glacial rivers. DOM in outflow samples from Russell Glacier exhibited a high degree of similarity,

whereas Svalbard rivers exhibited a high dissimilarity to both Russell Glacier outflow and to each other. Supraglacial samples from both regions were more similar to each other than to their respective outflow samples, suggesting similar sources and processes in the supraglacial environments. When data from High Mountain Asia are also included, glacially derived DOM is particularly enriched in bioavailable aliphatic and peptide-like formulae.

The contribution of bioavailable organic matter to downstream environments may be enhanced by a positive feedback loop driven by ice-sheet darkening. In the supraglacial environment, particularly in the "dark zone" of the GrIS, light absorbing material enhances melt of the ice sheet (Tedstone et al., 2017). Net autochthony (i.e., production outweighs respiration) can occur in both cryoconite holes and bare ice on the ice sheet surface (Anesio et al., 2010; Williamson et al., 2018). In cryoconite holes in the polar regions, bacterial doubling time can be < 10 days, providing a modern source of accumulating organic matter in the supraglacial environment (Anesio et al., 2010) in addition to dust from deposition (Wientjes et al., 2017). Cryoconite holes comprise a small cumulative area of the ablation zone, whereas glacier algae grow over a much larger fraction of the ice surface (Cook et al., 2020). Irradiance levels on the GrIS are currently rising due to decreasing cloud cover (Hofer et al., 2017), and algal density is higher in high melt years (Cook et al., 2020), both of which contribute to increased glacier mass loss. Thus, as algae and potential deposition act as a source of bioavailable organic matter, the concomitant increase in the amount and distribution of light absorbing material on the surface of the GrIS will enhance melting and further production of bioavailable organic matter. Glaciers in Greenland and Svalbard are projected to continue to lose mass throughout the 21st century (Radić et al., 2014). Depending on the climate scenario, periphery glaciers in Greenland are projected to exhibit 30–40 % glacier ice mass loss, which constitutes 12–20 mm sea-level equivalents, whereas Svalbard glaciers are projected to shrink by 60–65 % and contribute 12–16 mm sea-level equivalents by 2100 (Radić et al., 2014). Additionally, runoff from GrIS glaciers is projected to nearly double by 2100 (Muntjewerf et al., 2020). Even without an increase of microbially produced organic matter on glacier surfaces, the increase in glacier mass loss will reintroduce an additional ~15 Tg of DOC by 2050, on top of the ~30 Tg of DOC from current annual turnover, from a sequestered pool into the contemporary carbon cycle (Hood et al., 2015). Thus, as glaciers continue to lose mass throughout the 21st century, increasing contributions of bioavailable DOM to downstream environments are expected.

## Data Availability Statement

Data can be found in Tables 1–3 and are available through EarthChem (https://doi.org/10.26022/IEDA/111768) (Kellerman et al., 2021).

**Acknowledgments**
The authors would like to thank P. Zito for help with sample and data processing. We thank the Dutch Scientific Research Expedition Edgeøya Svalbard (SEES) in August 2015, as well as the Arctic Centre from the University of Groningen (The Netherlands), and the crew of the Ortelius. We thank the Kangerlussuaq International Science Support facility for help with logistics planning and implementation. We acknowledge funding from the US National Science Foundation grant OCE-1333157 to R.G.M.S. A portion of this work was performed at the National High Magnetic Field Laboratory ICR User Facility, which is supported by the National Science Foundation Division of Chemistry through DMR 11-57490 and DMR 1644779 and the State of Florida. Discharge data from Watson River in West Greenland were gathered by the University of Copenhagen (2006-2013) and the Geological Survey of Denmark and Greenland (2014-present).

## References

Aitkenhead, J. A., & McDowell, W. H. (2000). Soil C:N ratio as a predictor of annual riverine DOC flux at local and global scales. *Global Biogeochemical Cycles*, *14*(1), 127–138. https://doi.org/10.1029/1999gb900083

Anesio, A. M., Lutz, S., Chrismas, N. A. M., & Benning, L. G. (2017). The microbiome of glaciers and ice sheets. *NPJ Biofilms Microbiomes*, *3*, 10. https://doi.org/10.1038/s41522-017-0019-0

Anesio, A. M., Sattler, B., Foreman, C. M., Telling, J., HODSON, A., Tranter, M., & Psenner, R. (2010). Carbon fluxes through bacterial communities on glacier surfaces. *Annals of Glaciology*, *51*(56), 32–40. https://doi.org/10.3189/172756411795932092

Battin, T. J., Luyssaert, S., Kaplan, L. A., Aufdenkampe, A. K., Richter, A., & Tranvik, L. J. (2009). The boundless carbon cycle. *Nature Geoscience*, *2*(9), 598–600. https://doi.org/10.1038/ngeo618

Bayer, B., Hansman, R. L., Bittner, M. J., Noriega-Ortega, B. E., Niggemann, J., Dittmar, T., & Herndl, G. J. (2019). Ammonia-oxidizing archaea release a suite of organic compounds potentially fueling prokaryotic heterotrophy in the ocean. *Environmental Microbiology*, *21*(11), 4062–4075. https://doi.org/10.1111/1462-2920.14755

Beaton, A. D., Wadham, J. L., Hawkings, J., Bagshaw, E. A., Lamarche-Gagnon, G., Mowlem, M. C., & Tranter, M. (2017). High-resolution in situ measurement of nitrate in runoff from the Greenland ice sheet. *Environmental Science & Technology*, *51*(21), 12518–12527. https://doi.org/10.1021/acs.est.7b03121

Bhatia, M. P., Das, S. B., Longnecker, K., Charette, M. A., & Kujawinski, E. B. (2010). Molecular characterization of dissolved organic matter associated with the Greenland ice sheet. *Geochimica et Cosmochimica Acta*, *74*(13), 3768–3784. https://doi.org/10.1016/j.gca.2010.03.035

Bhatia, M. P., Das, S. B., Xu, L., Charette, M. A., Wadham, J. L., & Kujawinski, E. B. (2013). Organic carbon export from the Greenland ice sheet. *Geochimica et Cosmochimica Acta*, *109*, 329–344. https://doi.org/10.1016/j.gca.2013.02.006

Bittar, T. B., Vieira, A. A. H., Stubbins, A., & Mopper, K. (2015). Competition between photochemical and biological degradation of dissolved organic matter from the cyanobacteria Microcystis aeruginosa. *Limnology & Oceanography*, *60*(4), 1172–1194. https://doi.org/10.1002/lno.10090

Blakney, G. T., Hendrickson, C. L., & Marshall, A. G. (2011). Predator data station: A fast data acquisition system for advanced FT-ICR MS experiments. *International Journal of Mass Spectrometry*, *306*(2–3), 246–252. https://doi.org/10.1016/j.ijms.2011.03.009
Bouysse, P. (2014). *Geological map of the world at 1: 35 000 000* (3rd ed.). Paris, France: CCGM- CGMW.
Braithwaite, R. J. (1995). Positive degree-day factors for ablation on the Greenland ice sheet studied by energy-balance modelling. *Journal of Glaciology*, *41*(137), 153–160. https://doi.org/10.3189/S0022143000017846
Carrivick, J. L., & Quincey, D. J. (2014). Progressive increase in number and volume of ice-marginal lakes on the western margin of the Greenland ice sheet. *Global and Planetary Change*, *116*, 156–163. https://doi.org/10.1016/j.gloplacha.2014.02.009
Casas-Ruiz, J. P., Spencer, R. G. M., Guillemette, F., von Schiller, D., Obrador, B., Podgorski, D. C., et al. (2020). Delineating the continuum of dissolved organic matter in temperate river networks. *Global Biogeochemical Cycles*, *34*, e2019GB006495. https://doi.org/10.1029/2019GB006495
CAVM Team. (2003). *Circumpolar Arctic vegetation map. Scale 1:7,500,000. Conservation of Arctic Flora and Fauna (CAFF) Map No. 1*. Anchorage, Alaska: U.S. Fish and Wildlife Service.
Chen, M., Li, C., Zeng, C., Zhang, F., Raymond, P. A., & Hur, J. (2019). Immobilization of relic anthropogenic dissolved organic matter from alpine rivers in the Himalayan-Tibetan Plateau in winter. *Water Research*, *160*, 97–106. https://doi.org/10.1016/j.watres.2019.05.052
Cook, J. M., Hodson, A., Telling, J., Anesio, A., Irvine-Fynn, T., & Bellas, C. (2010). The mass–area relationship within cryoconite holes and its implications for primary production. *Annals of Glaciology*, *51*(56), 106–110. https://doi.org/10.3189/172756411795932038
Cook, J. M., Tedstone, A. J., Williamson, C., McCutcheon, J., Hodson, A. J., Dayal, A., et al. (2020). Glacier algae accelerate melt rates on the south-western Greenland Ice Sheet. *The Cryosphere*, *14*(1), 309–330. https://doi.org/10.5194/tc-14-309-2020
Corilo, Y. (2015). *EnviroOrg*: Florida State University.
Cowton, T., Nienow, P., Bartholomew, I., Sole, A., & Mair, D. (2012). Rapid erosion beneath the Greenland ice sheet. *Geology*, *40*(4), 343–346. https://doi.org/10.1130/g32687.1
D'Andrilli, J., Cooper, W. T., Foreman, C. M., & Marshall, A. G. (2015). An ultrahigh-resolution mass spectrometry index to estimate natural organic matter lability. *Rapid Communications in Mass Spectrometry*, *29*(24), 2385–2401. https://doi.org/10.1002/rcm.7400
Dial, R. J., Ganey, G. Q., & Skiles, S. M. (2018). What color should glacier algae be? An ecological role for red carbon in the cryosphere. *FEMS Microbiology Ecology*, *94*(3). https://doi.org/10.1093/femsec/fiy007
Dittmar, T., Koch, B., Hertkorn, N., & Kattner, G. (2008). A simple and efficient method for the solid-phase extraction of dissolved organic matter (SPE-DOM) from seawater. *Limnology and Oceanography: Methods*, *6*, 230–235. https://doi.org/10.4319/lom.2008.6.230
Findlay, S., & Sinsabaugh, R. L. (Eds.), (2003). *Aquatic ecosystems: Interactivity of dissolved organic matter*: Elsevier.
Fiore, C. L., Longnecker, K., Kido Soule, M. C., & Kujawinski, E. B. (2015). Release of ecologically relevant metabolites by the cyanobacterium Synechococcus elongates CCMP 1631. *Environmental Microbiology*, *17*(10), 3949–3963. https://doi.org/10.1111/1462-2920.12899
Hansell, D., Carlson, C., Repeta, D., & Schlitzer, R. (2009). Dissolved organic matter in the Ocean: A controversy stimulates new insights. *Oceanography*, *22*(4), 202–211. https://doi.org/10.5670/oceanog.2009.109
Hatton, J. E., Hendry, K. R., Hawkings, J. R., Wadham, J. L., Kohler, T. J., Stibal, M., et al. (2019). Investigation of subglacial weathering under the Greenland Ice Sheet using silicon isotopes, *Geochimica et Cosmochimica Acta*, *247*, 191–206. https://doi.org/10.1016/j.gca.2018.12.033
Hawkes, J. A., D'Andrilli, J., Agar, J. N., Barrow, M. P., Berg, S. M., Catalan, N., et al. (2020). An international laboratory comparison of dissolved organic matter composition by high resolution mass spectrometry: Are we getting the same answer? *Limnology and Oceanography: Methods*, *18*(6), 235–258. https://doi.org/10.1002/lom3.10364
Hawkings, J. R., Wadham, J. L., Benning, L. G., Hendry, K. R., Tranter, M., Tedstone, A., et al. (2017). Ice sheets as a missing source of silica to the polar oceans. *Nature Communications*, *8*, 14198. https://doi.org/10.1038/ncomms14198
Hemingway, J. D., Spencer, R. G. M., Podgorski, D. C., Zito, P., Sen, I. S., & Galy, V. V. (2019). Glacier meltwater and monsoon precipitation drive Upper Ganges Basin dissolved organic matter composition. *Geochimica et Cosmochimica Acta*, *244*, 216–228. https://doi.org/10.1016/j.gca.2018.10.012
Hendrickson, C. L., Quinn, J. P., Kaiser, N. K., Smith, D. F., Blakney, G. T., Chen, T., et al. (2015). 21 Tesla Fourier transform ion cyclotron resonance mass spectrometer: A national resource for ultrahigh resolution mass analysis. *Journal of the American Society for Mass Spectrometry*, *26*(9), 1626–1632. https://doi.org/10.1007/s13361-015-1182-2
Hertkorn, N., Benner, R., Frommberger, M., Schmitt-Kopplin, P., Witt, M., Kaiser, K., et al. (2006). Characterization of a major refractory component of marine dissolved organic matter. *Geochimica et Cosmochimica Acta*, *70*(12), 2990–3010. https://doi.org/10.1016/j.gca.2006.03.021
Hertkorn, N., Ruecker, C., Meringer, M., Gugisch, R., Frommberger, M., Perdue, E. M., et al. (2007). High-precision frequency measurements: indispensable tools at the core of the molecular-level analysis of complex systems. *Analytical and Bioanalytical Chemistry*, *389*(5), 1311–1327. https://doi.org/10.1007/s00216-007-1577-4
Hodson, A., Anesio, A. M., Tranter, M., Fountain, A., Osborn, M., Priscu, J., et al. (2008). Glacial Ecosystems. *Ecological Monographs*, *78*(1), 41–67. https://doi.org/10.1890/07-0187.1
Hofer, S., Tedstone, A. J., Fettweis, X., & Bamber, J. L. (2017). Decreasing cloud cover drives the recent mass loss on the Greenland ice sheet. *Science Advances*, *3*(6), e1700584. https://doi.org/10.1126/sciadv.1700584
Holland, A. T., Williamson, C. J., Sgouridis, F., Tedstone, A. J., McCutcheon, J., Cook, J. M., et al. (2019). Dissolved organic nutrients dominate melting surface ice of the Dark Zone (Greenland ice sheet). *Biogeosciences*, *16*(16), 3283–3296. https://doi.org/10.5194/bg-16-3283-2019
Hood, E., Battin, T. J., Fellman, J., O'Neel, S., & Spencer, R. G. M. (2015). Storage and release of organic carbon from glaciers and ice sheets. *Nature Geoscience*, *8*(2), 91–96. https://doi.org/10.1038/ngeo2331
Hood, E., Fellman, J., Spencer, R. G., Hernes, P. J., Edwards, R., D'Amore, D., & Scott, D. (2009). Glaciers as a source of ancient and labile organic matter to the marine environment. *Nature*, *462*(7276), 1044–1047. https://doi.org/10.1038/nature08580
Institute, N. P. (2016). *Geological map of Svalbard (1:.250000)* (Data set): Norwegian Polar Institute. https://doi.org/10.21334/npolar.2016.616f7504
Irvine-Fynn, T. D. L., Hodson, A. J., Moorman, B. J., Vatne, G., & Hubbard, A. L. (2011). Polythermal glacier hydrology: A review. *Reviews of Geophysics*, *49*(4). https://doi.org/10.1029/2010rg000350
Jacobson, M. C., Hansson, H. C., Noone, K. J., & Charlson, R. J. (2000). Organic atmospheric aerosols: Review and state of the science. *Reviews of Geophysics*, *38*(2), 267–294. https://doi.org/10.1029/1998rg000045
Jordan, T. M., Williams, C. N., Schroeder, D. M., Martos, Y. M., Cooper, M. A., Siegert, M. J., et al. (2018). A constraint upon the basal water distribution and thermal state of the Greenland Ice Sheet from radar bed echoes. *The Cryosphere*, *12*(9), 2831–2854. https://doi.org/10.5194/tc-12-2831-2018

Kamga, A. W., Behar, F., & Hatcher, P. G. (2014). Quantitative analysis of long chain fatty acids present in a Type I kerogen using electrospray ionization Fourier transform ion cyclotron resonance mass spectrometry: Compared with BF(3)/MeOH methylation/GC-FID. *Journal of the American Society for Mass Spectrometry*, *25*(5), 880–890. https://doi.org/10.1007/s13361-014-0851-x

Kellerman, A. M., Arellano, A., Podgorski, D. C., Martin, E. E., Martin, J. B., Deuerling, K. M., et al. (2020a). Fundamental drivers of dissolved organic matter composition across an Arctic effective precipitation gradient. *Limnology & Oceanography*, *65*(6), 1217–1234. https://doi.org/10.1002/lno.11385

Kellerman, A. M., Dittmar, T., Kothawala, D. N., & Tranvik, L. J. (2014). Chemodiversity of dissolved organic matter in lakes driven by climate and hydrology. *Nature Communications*, *5*, 3804. https://doi.org/10.1038/ncomms4804

Kellerman, A. M., Guillemette, F., Podgorski, D. C., Aiken, G. R., Butler, K. D., & Spencer, R. G. M. (2018). Unifying concepts linking dissolved organic matter composition to persistence in aquatic ecosystems. *Environmental Science & Technology*, *52*(5), 2538–2548. https://doi.org/10.1021/acs.est.7b05513

Kellerman, A. M., Hawkings, J. R., Wadham, J. L., Kohler, T. J., Stibal, M., Grater, E. M., et al. (2020b). Glacier outflow dissolved organic matter as a window into seasonally changing carbon sources: Leverett Glacier, Greenland. *Journal of Geophysical Research: Biosciences*, *125*(4), e2019JG005161. https://doi.org/10.1029/2019JG005161

Kellerman, A. M., Kothawala, D. N., Dittmar, T., & Tranvik, L. J. (2015). Persistence of dissolved organic matter in lakes related to its molecular characteristics. *Nature Geoscience*, *8*(6), 454–457. https://doi.org/10.1038/ngeo2440

Kellerman, A. M., Vonk, J., McColaugh, S., Podgorski, D., van Winden, E., Hawkings, J., et al. (2021). Ultrahigh resolution mass spectrometry characterization of dissolved organic matter from glacial systems in Greenland and Svalbard. *Interdisciplinary Earth Data Alliance (IEDA)*. https://doi.org/10.26022/IEDA/111768

Knight, P. G., Waller, R. I., Patterson, C. J., Jones, A. P., & Robinson, Z. P. (2000). Glacier advance, ice-marginal lakes and routing of meltwater and sediment: Russell Glacier, Greenland. *Journal of Glaciology*, *46*(154), 423–426. https://doi.org/10.3189/172756500781833160

Koch, B. P., & Dittmar, T. (2006). From mass to structure: An aromaticity index for high-resolution mass data of natural organic matter. *Rapid Communications in Mass Spectrometry*, *20*(5), 926–932. https://doi.org/10.1002/rcm.2386

Koch, B. P., & Dittmar, T. (2016). From mass to structure: An aromaticity index for high-resolution mass data of natural organic matter. *Rapid Communications in Mass Spectrometry*, *30*(1), 250. https://doi.org/10.1002/rcm.7433

Kohler, T. J., Žárský, J. D., Yde, J. C., Lamarche-Gagnon, G., Hawkings, J. R., Tedstone, A. J., et al. (2017). Carbon dating reveals a seasonal progression in the source of particulate organic carbon exported from the Greenland Ice Sheet. *Geophysical Research Letters*, *44*(12), 6209–6217. https://doi.org/10.1002/2017gl073219

Lamarche-Gagnon, G., Wadham, J. L., Lollar, B. S., Arndt, S., Fietzek, P., Beaton, A. D., et al. (2019). Greenland melt drives continuous export of methane from the ice-sheet bed. *Nature*, *565*(7737), 73–77. https://doi.org/10.1038/s41586-018-0800-0

Lawson, E. C., Bhatia, M. P., Wadham, J. L., & Kujawinski, E. B. (2014). Continuous summer export of nitrogen-rich organic matter from the Greenland Ice Sheet inferred by ultrahigh resolution mass spectrometry. *Environmental Science & Technology*, *48*(24), 14248–14257. https://doi.org/10.1021/es501732h

Lawson, E. C., Wadham, J. L., Tranter, M., Stibal, M., Lis, G. P., Butler, C. E. H., et al. (2014). Greenland Ice Sheet exports labile organic carbon to the Arctic oceans. *Biogeosciences*, *11*(14), 4015–4028. https://doi.org/10.5194/bg-11-4015-2014

Levy, L. B., Larsen, N. K., Davidson, T. A., Strunk, A., Olsen, J., & Jeppesen, E. (2017). Contrasting evidence of Holocene ice margin retreat, south-western Greenland. *Journal of Quaternary Science*, *32*(5), 604–616. https://doi.org/10.1002/jqs.2957

Liao, H. G., Zherebetskyy, D., Xin, H., Czarnik, C., Ercius, P., Elmlund, H., et al. (2014). Nanoparticle growth. Facet development during platinum nanocube growth. *Science*, *345*(6199), 916–919. https://doi.org/10.1126/science.1253149

Lindbäck, K., Pettersson, R., Hubbard, A. L., Doyle, S. H., As, D., Mikkelsen, A. B., & Fitzpatrick, A. A. (2015). Subglacial water drainage, storage, and piracy beneath the Greenland ice sheet. *Geophysical Research Letters*, *42*(18), 7606–7614. https://doi.org/10.1002/2015gl065393

Longnecker, K., Kido Soule, M. C., & Kujawinski, E. B. (2015). Dissolved organic matter produced by Thalassiosira pseudonana. *Marine Chemistry*, *168*, 114–123. https://doi.org/10.1016/j.marchem.2014.11.003

MacGregor, J. A., Fahnestock, M. A., Catania, G. A., Aschwanden, A., Clow, G. D., Colgan, W. T., et al. (2016). A synthesis of the basal thermal state of the Greenland ice sheet. *Journal of Geophysical Research: Earth Surface*, *121*(7), 1328–1350. https://doi.org/10.1002/2015JF003803

Mazzoleni, L. R., Saranjampour, P., Dalbec, M. M., Samburova, V., Hallar, A. G., Zielinska, B., et al. (2012). Identification of water-soluble organic carbon in non-urban aerosols using ultrahigh-resolution FT-ICR mass spectrometry: Organic anions. *Environmental Chemistry*, *9*(3), 285. https://doi.org/10.1071/en11167

Mladenov, N., Reche, I., Olmo, F. J., Lyamani, H., & Alados-Arboledas, L. (2010). Relationships between spectroscopic properties of high-altitude organic aerosols and Sun photometry from ground-based remote sensing. *Journal of Geophysical Research*, *115*. https://doi.org/10.1029/2009jg000991

Mladenov, N., Sommaruga, R., Morales-Baquero, R., Laurion, I., Camarero, L., Dieguez, M. C., et al. (2011). Dust inputs and bacteria influence dissolved organic matter in clear alpine lakes. *Nature Communications*, *2*, 405. https://doi.org/10.1038/ncomms1411

Moroni, B., Arnalds, O., Dagsson-Waldhauserová, P., Crocchianti, S., Vivani, R., & Cappelletti, D. (2018). Mineralogical and chemical records of icelandic dust sources upon Ny-Ålesund (Svalbard Islands). *Frontiers in Earth Science*, *6*. https://doi.org/10.3389/feart.2018.00187

Mostovaya, A., Hawkes, J. A., Koehler, B., Dittmar, T., & Tranvik, L. J. (2017). Emergence of the reactivity continuum of organic matter from kinetics of a multitude of individual molecular constituents. *Environmental Science & Technology*, *51*(20), 11571–11579. https://doi.org/10.1021/acs.est.7b02876

Muntjewerf, L., Petrini, M., Vizcaino, M., da Silva, C. E., Sellevold, R., Scherrenberg, M. D. W., et al. (2020). Greenland ice sheet contribution to 21st century sea level rise as simulated by the coupled CESM2.1-CISM2.1. *Geophysical Research Letters*, *47*(9). https://doi.org/10.1029/2019gl086836

Musilova, M., Tranter, M., Wadham, J., Telling, J., Tedstone, A., & Anesio, A. M. (2017). Microbially driven export of labile organic carbon from the Greenland ice sheet. *Nature Geoscience*, *10*(5), 360–365. https://doi.org/10.1038/ngeo2920

Nicholes, M. J., Williamson, C. J., Tranter, M., Holland, A., Poniecka, E., Yallop, M. L., et al. (2019). Bacterial dynamics in supraglacial habitats of the Greenland ice sheet. *Frontiers in Microbiology*, *10*, 1366. https://doi.org/10.3389/fmicb.2019.01366

Noriega-Ortega, B. E., Wienhausen, G., Mentges, A., Dittmar, T., Simon, M., & Niggemann, J. (2019). Does the chemodiversity of bacterial exometabolomes sustain the chemodiversity of marine dissolved organic matter? *Frontiers in Microbiology*, *10*, 215. https://doi.org/10.3389/fmicb.2019.00215

O'Donnell, E. C., Wadham, J. L., Lis, G. P., Tranter, M., Pickard, A. E., Stibal, M., et al. (2016). Identification and analysis of low-molecular-weight dissolved organic carbon in subglacial basal ice ecosystems by ion chromatography. *Biogeosciences*, *13*(12), 3833–3846. https://doi.org/10.5194/bg-13-3833-2016

Oksanen, J., Blanchet, F. G., Kindt, R., Legender, P., Minchin, P. R., O'Hara, R. B., et al. (2011). *Vegan: Community ecology package*. R package version 2.0-0, edited.

Osterholz, H., Dittmar, T., & Niggemann, J. (2014). Molecular evidence for rapid dissolved organic matter turnover in Arctic fjords. *Marine Chemistry*, *160*, 1–10. https://doi.org/10.1016/j.marchem.2014.01.002

Osterholz, H., Kirchman, D. L., Niggemann, J., & Dittmar, T. (2016). Environmental drivers of dissolved organic matter molecular composition in the Delaware Estuary. *Frontiers in Earth Science*, *4*, 95. https://doi.org/10.3389/feart.2016.00095

Paulsen, M. L., Seuthe, L., Reigstad, M., Larsen, A., Cape, M. R., & Vernet, M. (2018). Asynchronous accumulation of organic carbon and nitrogen in the atlantic gateway to the Arctic Ocean. *Frontiers in Marine Science*, *5*. https://doi.org/10.3389/fmars.2018.00416

Powers, L. C., Hertkorn, N., McDonald, N., Schmitt-Kopplin, P., Del Vecchio, R., Blough, N. V., & Gonsior, M. (2019). Sargassumsp. Act as a large regional source of marine dissolved organic carbon and polyphenols. *Global Biogeochemical Cycles*, *33*(11), 1423–1439. https://doi.org/10.1029/2019gb006225

R Core Team. (2015). *R: A language and environment for statistical computing*. Vienna, Austria: R Foundation for Statistical Computing.

Radić, V., Bliss, A., Beedlow, A. C., Hock, R., Miles, E., & Cogley, J. G. (2014). Regional and global projections of twenty-first century glacier mass changes in response to climate scenarios from global climate models. *Climate Dynamics*, *42*, 37–58. https://doi.org/10.1007/s00382-013-1719-7

Remias, D., Schwaiger, S., Aigner, S., Leya, T., Stuppner, H., & Lutz, C. (2012). Characterization of an UV- and VIS-absorbing, purpurogallin-derived secondary pigment new to algae and highly abundant in Mesotaenium berggrenii (Zygnematophyceae, Chlorophyta), an extremophyte living on glaciers. *FEMS Microbiology Ecology*, *79*(3), 638–648. https://doi.org/10.1111/j.1574-6941.2011.01245.x

Rennermalm, A. K., Moustafa, S. E., Mioduszewski, J., Chu, V. W., Forster, R. R., Hagedorn, B., et al. (2013). Understanding Greenland ice sheet hydrology using an integrated multi-scale approach. *Environmental Research Letters*, *8*(1), 015017. https://doi.org/10.1088/1748-9326/8/1/015017

Rennermalm, A. K., Smith, L. C., Chu, V. W., Forster, R. R., Box, J. E., & Hagedorn, B. (2012). Proglacial river stage, discharge, and temperature datasets from the Akuliarusiarsuup Kuua River northern tributary, Southwest Greenland, 2008–2011. *Earth System Science Data*, *4*(1), 1–12. https://doi.org/10.5194/essd-4-1-2012

Riedel, T., Biester, H., & Dittmar, T. (2012). Molecular fractionation of dissolved organic matter with metal salts. *Environmental Science & Technology*, *46*(8), 4419–4426. https://doi.org/10.1021/es203901u

Riedel, T., Zark, M., Vähätalo, A. V., Niggemann, J., Spencer, R. G. M., Hernes, P. J., & Dittmar, T. (2016). Molecular signatures of biogeochemical transformations in dissolved organic matter from ten world rivers. *Frontiers in Earth Science*, *4*. https://doi.org/10.3389/feart.2016.00085

Romano, S., Dittmar, T., Bondarev, V., Weber, R. J., Viant, M. R., & Schulz-Vogt, H. N. (2014). Exo-metabolome of Pseudovibrio sp. FO-BEG1 analyzed by ultra-high resolution mass spectrometry and the effect of phosphate limitation. *PLoS One*, e96038. *9*(5). https://doi.org/10.1371/journal.pone.0096038

Salmon, E., Behar, F., & Hatcher, P. G. (2011). Molecular characterization of Type I kerogen from the Green River Formation using advanced NMR techniques in combination with electrospray ionization/ultrahigh resolution mass spectrometry. *Organic Geochemistry*, *42*(4), 301–315. https://doi.org/10.1016/j.orggeochem.2010.12.007

Schmidt, M. W., Torn, M. S., Abiven, S., Dittmar, T., Guggenberger, G., Janssenes, I. A., et al. (2011). Persistence of soil organic matter as an ecosystem property. *Nature*, *478*(7367), 49–56. https://doi.org/10.1038/nature10386

Seidel, M., Yager, P. L., Ward, N. D., Carpenter, E. J., Gomes, H. R., Krusche, A. V., et al. (2015). Molecular-level changes of dissolved organic matter along the Amazon River-to-ocean continuum. *Marine Chemistry*, *177*, 218–231. https://doi.org/10.1016/j.marchem.2015.06.019

Sevestre, H., Benn, D. I., Hulton, N. R. J., & Bælum, K. (2015). Thermal structure of Svalbard glaciers and implications for thermal switch models of glacier surging. *Journal of Geophysical Research: Earth Surface*, *120*(10), 2220–2236. https://doi.org/10.1002/2015jf003517

Singer, G. A., Fasching, C., Wilhelm, L., Niggemann, J., Steier, P., Dittmar, T., & Battin, T. J. (2012). Biogeochemically diverse organic matter in Alpine glaciers and its downstream fate. *Nature Geoscience*, *5*(10), 710–714. https://doi.org/10.1038/ngeo1581

Smith, D. F., Podgorski, D. C., Rodgers, R. P., Blakney, G. T., & Hendrickson, C. L. (2018). 21 Tesla FT-ICR mass spectrometer for ultrahigh-resolution analysis of complex organic mixtures. *Analytical Chemistry*, *90*(3), 2041–2047. https://doi.org/10.1021/acs.analchem.7b04159

Smith, H. J., Foster, R. A., McKnight, D. M., Lisle, J. T., Littmann, S., Kuypers, M. M. M., & Foreman, C. M. (2017). Microbial formation of labile organic carbon in Antarctic glacial environments. *Nature Geoscience*, *10*(5), 356–359. https://doi.org/10.1038/ngeo2925

Spencer, R. G. M., Butler, K. D., & Aiken, G. R. (2012). Dissolved organic carbon and chromophoric dissolved organic matter properties of rivers in the USA. *Journal of Geophysical Research*, *117*(G3). https://doi.org/10.1029/2011jg001928

Spencer, R. G. M., Guo, W., Raymond, P. A., Dittmar, T., Hood, E., Fellman, J., & Stubbins, A. (2014). Source and biolability of ancient dissolved organic matter in glacier and lake ecosystems on the Tibetan Plateau. *Geochimica et Cosmochimica Acta*, *142*, 64–74. https://doi.org/10.1016/j.gca.2014.08.006

Spencer, R. G. M., Mann, P. J., Dittmar, T., Eglinton, T. I., McIntyre, C., Holmes, R. M., et al. (2015). Detecting the signature of permafrost thaw in Arctic rivers. *Geophysical Research Letters*, *42*(8), 2830–2835. https://doi.org/10.1002/2015gl063498

Spencer, R. G. M., Vermilyea, A., Fellman, J., Raymond, P., Stubbins, A., Scott, D., & Hood, E. (2014). Seasonal variability of organic matter composition in an Alaskan glacier outflow: Insights into glacier carbon sources. *Environmental Research Letters*, *9*(5). https://doi.org/10.1088/1748-9326/9/5/055005

Stenson, A. C., Marshall, A. G., & Cooper, W. T. (2003). Exact masses and chemical formulas of individual Suwannee River fulvic acids from ultrahigh resolution electrospray ionization Fourier transform ion cyclotron resonance mass spectra. *Analytical Chemistry*, *75*(6), 1275–1284. https://doi.org/10.1021/ac026106p

Stibal, M., Gozdereliler, E., Cameron, K. A., Box, J. E., Stevens, I. T., Gokul, J. A., et al. (2015). Microbial abundance in surface ice on the Greenland ice sheet. *Frontiers in Microbiology*, *6*, 225. https://doi.org/10.3389/fmicb.2015.00225

Stibal, M., Schostag, M., Cameron, K. A., Hansen, L. H., Chandler, D. M., Wadham, J. L., & Jacobsen, C. S. (2015). Different bulk and active bacterial communities in cryoconite from the margin and interior of the Greenland ice sheet. *Environmental Microbiology Reports*, *7*(2), 293–300. https://doi.org/10.1111/1758-2229.12246

Stubbins, A., & Dittmar, T. (2015). Illuminating the deep: Molecular signatures of photochemical alteration of dissolved organic matter from North Atlantic Deep Water. *Marine Chemistry*, *177*, 318–324. https://doi.org/10.1016/j.marchem.2015.06.020

Stubbins, A., Hood, E., Raymond, P. A., Aiken, G. R., Sleighter, R. L., Hernes, P. J., et al. (2012). Anthropogenic aerosols as a source of ancient dissolved organic matter in glaciers. *Nature Geoscience*, *5*(3), 198–201. https://doi.org/10.1038/ngeo1403

Stubbins, A., Spencer, R. G. M., Chen, H., Hatcher, P. G., Mopper, K., Hernes, P. J., et al. (2010). Illuminated darkness: Molecular signatures of Congo River dissolved organic matter and its photochemical alteration as revealed by ultrahigh precision mass spectrometry. *Limnology & Oceanography*, *55*(4), 1467–1477. https://doi.org/10.4319/lo.2010.55.4.1467

Takeuchi, N., Kohshima, S., & Seko, K. (2018). Structure, formation, and darkening process of albedo-reducing material (cryoconite) on a Himalayan Glacier: A granular algal mat growing on the glacier. *Arctic, Antarctic, and Alpine Research*, *33*(2), 115–122. https://doi.org/10.1080/15230430.2001.12003413

Tedstone, A. J., Bamber, J. L., Cook, J. M., Williamson, C. J., Fettweis, X., Hodson, A. J., & Tranter, M. (2017). Dark ice dynamics of the south-west Greenland ice sheet. *The Cryosphere*, *11*(6), 2491–2506. https://doi.org/10.5194/tc-11-2491-2017

Telling, J., Anesio, A. M., Tranter, M., Stibal, M., Hawkings, J., Irvine-Fynn, T., et al. (2012). Controls on the autochthonous production and respiration of organic matter in cryoconite holes on high Arctic glaciers. *Journal of Geophysical Research*, *117*(G1). https://doi.org/10.1029/2011jg001828

van As, D., Bech Mikkelsen, A., Holtegaard Nielsen, M., Box, J. E., Claesson Liljedahl, L., Lindbäck, K., et al. (2017). Hypsometric amplification and routing moderation of Greenland ice sheet meltwater release. *The Cryosphere*, *11*(3), 1371–1386. https://doi.org/10.5194/tc-11-1371-2017

van As, D., Hasholt, B., Ahlstrom, A. P., Box, J. E., Colgan, C. J., Fausto, W., et al. (2019). *Programme for monitoring of the Greenland ice sheet (PROMICE): Watson river discharge. Version: v01*: Geological Survey of Denmark and Greenland. https://doi.org/10.22008/promice/data/watson_river_discharge

Wadham, J. L., Hawkings, J. R., Tarasov, L., Gregoire, L. J., Spencer, R. G. M., Gutjahr, M., et al. (2019). Ice sheets matter for the global carbon cycle. *Nature Communications*, *10*(1), 3567. https://doi.org/10.1038/s41467-019-11394-4

Wagner, S., Riedel, T., Niggemann, J., Vahatalo, A. V., Dittmar, T., & Jaffe, R. (2015). Linking the Molecular Signature of Heteroatomic Dissolved Organic Matter to Watershed Characteristics in World Rivers. *Environmental science & technology*, *49*(23), 13798–13806. https://doi.org/10.1021/acs.est.5b00525

Wal, R. S. W. v. d., & Russell, A. J. (1994). A comparison of energy balance calculations, measured ablation and meltwater runoff near Søndre Strømfjord, West Greenland. *Global and Planetary Change*, *9*, 29–38. https://doi.org/10.1016/0921-8181(94)90005-1

Wienhausen, G. M. (2018). *Linking the exometabolome of selected organisms of the Roseobacter group to marine dissolved organic matter—A microbiological perspective* (p. 155). Carl von Ossietzky Universität Oldenburg.

Wienhausen, G. M., Noriega-Ortega, B. E., Niggemann, J., Dittmar, T., & Simon, M. (2017). The Exometabolome of two model strains of the roseobacter group: A marketplace of microbial metabolites. *Frontiers in Microbiology*, *8*, 1985. https://doi.org/10.3389/fmicb.2017.01985

Wientjes, I. G. M., Van de Wal, R. S. W., Reichart, G. J., Sluijs, A., & Oerlemans, J. (2011). Dust from the dark region in the western ablation zone of the Greenland ice sheet. *The Cryosphere*, *5*(3), 589–601. https://doi.org/10.5194/tc-5-589-2011

Wientjes, I. G. M., Van De Wal, R. S. W., Schwikowski, M., Zapf, A., Fahrni, S., & Wacker, L. (2017). Carbonaceous particles reveal that Late Holocene dust causes the dark region in the western ablation zone of the Greenland ice sheet. *Journal of Glaciology*, *58*(210), 787–794. https://doi.org/10.3189/2012JoG11J165

Williamson, C. J., Anesio, A. M., Cook, J., Tedstone, A., Poniecka, E., Holland, A., et al. (2018). Ice algal bloom development on the surface of the Greenland ice sheet. *FEMS Microbiology Ecology*, *94*(3), fiy025. https://doi.org/10.1093/femsec/fiy025

Williamson, C. J., Cameron, K. A., Cook, J. M., Zarsky, J. D., Stibal, M., & Edwards, A. (2019). Glacier algae: A dark past and a darker future. *Frontiers in Microbiology*, *10*, 524. https://doi.org/10.3389/fmicb.2019.00524

Williamson, C. J., Cook, J., Tedstone, A., Yallop, M., McCutcheon, J., Poniecka, E., et al. (2020). Algal photophysiology drives darkening and melt of the Greenland ice sheet. *Proceedings of the National Academy of Sciences of the United States of America*, *117*(11), 5694–5705. https://doi.org/10.1073/pnas.1918412117

Wozniak, A. S., Bauer, J. E., Sleighter, R. L., Dickhut, R. M., & Hatcher, P. G. (2008). Technical Note: Molecular characterization of aerosol-derived water soluble organic carbon using ultrahigh resolution electrospray ionization Fourier transform ion cyclotron resonance mass spectrometry. *Atmospheric Chemistry and Physics*, *8*, 5099–5111. https://doi.org/10.5194/acp-8-5099-2008

Zherebker, A., Kim, S., Schmitt-Kopplin, P., Spencer, R. G. M., Lechtenfeld, O., Podgorski, D. C., et al. (2020). Interlaboratory comparison of humic substances compositional space as measured by Fourier transform ion cyclotron resonance mass spectrometry (IUPAC Technical Report). *Pure and Applied Chemistry*, *92*(9), 1447–1467. https://doi.org/10.1515/pac-2019-0809

Zhou, L., Zhou, Y., Hu, Y., Cai, J., Liu, X., Bai, C., et al. (2019). Microbial production and consumption of dissolved organic matter in glacial ecosystems on the Tibetan Plateau. *Water Research*, *160*, 18–28. https://doi.org/10.1016/j.watres.2019.05.048

Zhou, Y., Zhou, L., He, X., Jang, K-S., Yao, X., Hu, Y., et al. (2019). Variability in dissolved organic matter composition and biolability across gradients of glacial coverage and distance from glacial terminus on the Tibetan Plateau. *Environmental Science & Technology*, *53*(21), 12207–12217. https://doi.org/10.1021/acs.est.9b03348